Examensarbete
TVVR 12/5015

Effect on future hydropower potential from use of different bias correction methods for three Swedish river basins

Olof Nilsson
Tobias Renlund

Division of Water Resources Engineering
Department of Building and Environmental Technology
Lund University

Avdelningen för Teknisk Vattenresurslära
TVVR-12/5015

ISSN-1101-9824

Effect on future hydropower potential from use of different bias correction methods for three Swedish river basins

Olof Nilsson

Tobias Renlund

Abstract

Hydropower is responsible for approximately 45 % of the Swedish annual electricity production making it an important constituent of the Swedish energy market. This master thesis serves to evaluate how the use of three different bias correction methods and the delta change approach effect the predicted future hydropower production in Lule, Skellefte and Dal river basin.

The study includes one global emission scenario, A1B, two global climate models (GCMs), ECHAM5 and HADCM3, and one regional climate model (RCM), RCA3. The Thomson Reuters Point Carbon in-house HBV energy model was used to evaluate the results.

Results indicated an increase in both precipitation and inflow to the hydropower systems in the future. Spring inflow (week 16-28) increased in Lule and decreased in Skellefte and Dal. For all river basins the majority of the increase was distributer during August – March. Results also indicate earlier arrival of the spring flood in the future and spring peak inflow that remain constant for Lule and Skellefte and decrease for Dal. Temperature increases between 2.5-4.7 degrees.

It was concluded that the choice of bias correction method had great impact on the end result. Overall quantile mapping performed best and would be our recommendation for any application that did not focus solely on the mean changes. If only the mean changes in amount of precipitation was of interest delta change would be the best choice due to its simplicity.

Acknowledgments

We would like to begin by expressing our humble thanks to our supervisor at LTH professor Cintia Bertacchi Uvo, for your continued encouragement and excellent guidance throughout the course of this master thesis.

Thanks to Professor Rolf Larsson for making the time to be our examiner.

Thank you Marion Guegan, Thomson Reuters Point Carbon, and Erik Mårtensson, DHI for bestowing us so much of your time, sharing your experience and always providing good answers to our many questions. Your continued support and feedback throughout this project have helped improved the quality of our work and taught us many valuable lessons.

Lastly we would like to thank our teachers at LTH for providing such a high standard of education and our families and friends that helped make our time here such a memorable and enjoyable experience.

Abbreviations

Full name	Abbreviations
Delta change	DC
Mean value	MV
Mean value and variance	MVV
Quantile mapping	QM
Intergovernmental Panel on Climate Change	IPCC
Global Climate Model	GCM
Regional Climate Model	RCM

Keywords: Hydropower, climate change, bias correction method, spring flood, snowpack, peak flow

Contents

Figures

Tables

1 Introduction

The Intergovernmental Panel on Climate Change concluded with very high confidence in their latest report from 2007 that the net effect of human activities since 1750 has been one of warming (IPCC, 2007). During the past decades climate change has gone from being an unproven theory to being widely accepted. This has meant a lot of new considerations for government officials as well as the private sector.

With additional focus being put on climate change effects as a basis for future planning and decision-making, the importance of evaluating the climate models, their intended use and inherit uncertainties has increased. Global Climate Models (GCM) is the primary tool for understanding the future changes in global climate. However for local applications the GCM grid size (>200 km^2) is too large to give the necessary resolution to capture e.g. hydrological processes (Meehl et al., 2007). To address this problem Regional Climate Models (RCM) are used as a way of dynamically downscaling GCM results. Using the boundary conditions provided by the GCM, the RCM provides finer resolution and better representation of both geographical features and physical processes for a limited area (Yang et al., 2010).

1.1 Problem description

Modelling the complex interactions between atmosphere, oceans and biosphere is no easy task and every model is subject to some sort of systematic bias. An example is how regional climate models tend to have a number of wet days that is much higher than for the observed data. There are several reasons for this, predominantly the fact that the entire grid frame is always appointed the same precipitation value even if only a very small part of the grid was in fact affected by precipitation. As a consequence the total amount of precipitation is overestimated in the model, see example in Figure 1.

This means that typically using uncorrected data from the RCM as input to a hydrological model gives large deviations from observed data and measurements (Graham et al., 2007). This is where bias correction methods come in, to serve as an interface for data transfer from the RCM to the hydrological model (Madsen et al. 2010).

The reason to carry out bias correction can be seen in Figure 1 where we have the uncorrected output from the two climate scenarios ECHAM5-RCA3-A1B and HADCM3-RCA3-A1B. These two scenarios will hereafter be referred to as ECHAM and HADCM, since the emission scenario A1B and regional climate model RCA is the same in both cases.

Figure 1 show the uncorrected precipitation for both scenarios for the reference time period 1981-2005, the same period from which observed data is taken, if these scenarios were perfect they would give the same results as the observed values for this time period. This is however not the case, instead we see an overestimation of precipitation with between 5-120 %.

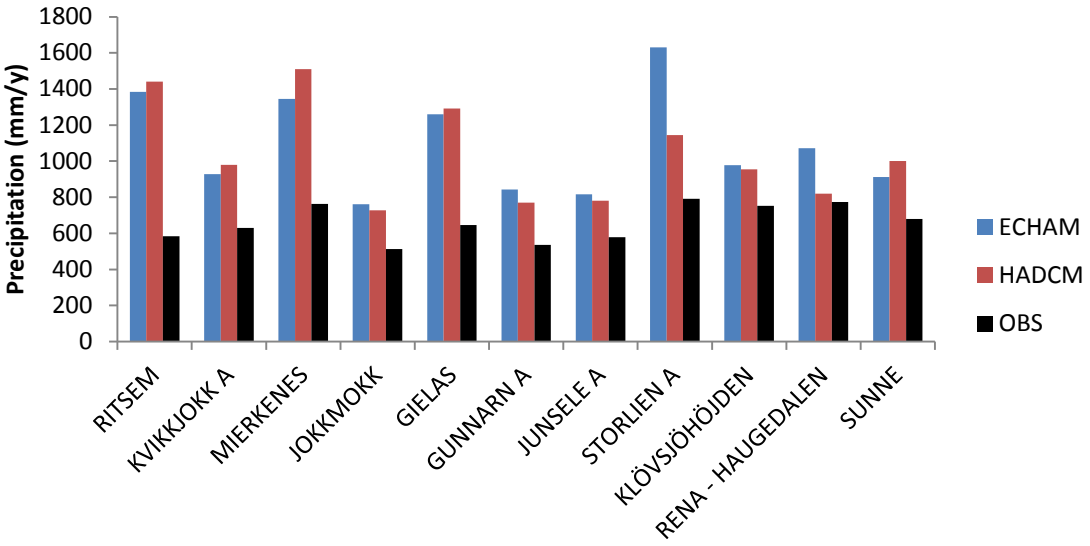

Figure 1 Uncorrected annual mean precipitation for ECHAM and HADCM for reference period compared to observed reference period. Stations are sorted on the x-axis from north (left) to south (right).

This is where bias correction methods come in, to serve as an interface for data transfer between the regional climate model and the hydrological model as can be seen in Figure 2.

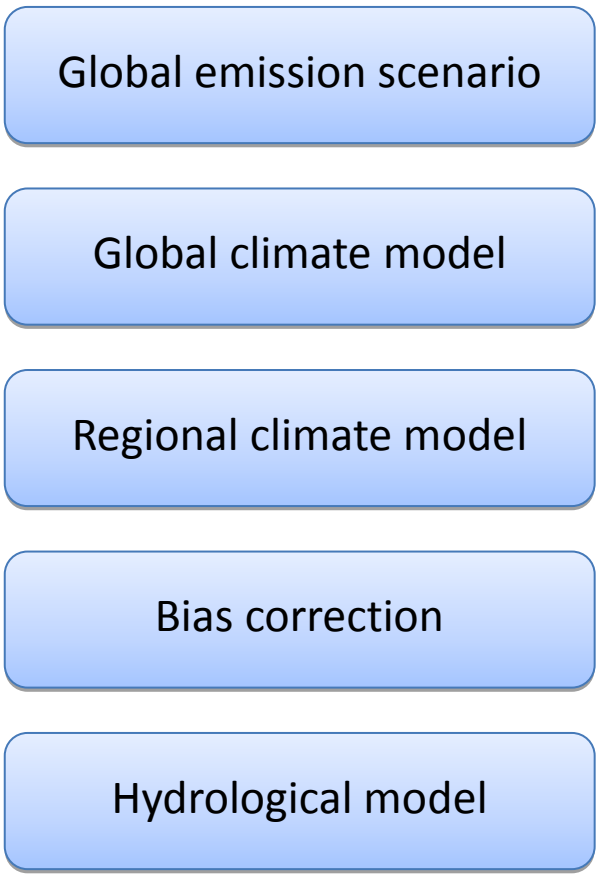

Figure 2 Schematic picture of the different steps when dealing with predictions of future climate for hydrological modeling applications.

Out of the four correction methods studied three out of four are classic bias correction methods in the sense that they use the model future output with applied correction factors to create the corrected future output. The fourth method is not technically a bias correction method since it uses observed climate as a baseline to create the future data series, but it is very commonly used and serves the same purpose e.g. Bergström et al., (2003), Andréasson et al., (2004) and Graham et. al, (2007). In the delta change method the difference between modelled future and modelled reference period is used to create change factors which are applied to the observed values. The methods are described in further detail in section 4.1-4.4.

1.2 Aim

This thesis project will compare three different bias correction methods as well as the commonly used Delta Change method and evaluate how the choice of method affects the end result on hydropower potential in three different Swedish river catchments. The correction methods will be applied on two different climate scenarios (ECHAM5-RCA3-A1B and HADCM3-RCA3-A1B) and two future time periods (2016-2040 and 2076-2100).

2 Background

2.1 Hydropower in Sweden

Hydropower is one of the major sources of energy in Sweden making up approximately 45% of the total annual electricity production (Swedish energy agency, 2008). The production is mainly concentrated to the northern parts of the country with hydropower stations in Norrland corresponding to close to 80% of the total production (Svensk energi, 2011). This can have a big effect on the future projections for hydropower production as many previous studies have shown that the distribution of precipitation increase due to climate change will vary between the northern and southern parts of the country (Graham et al., 2007).

2.2 River basins

Three different river basins were included in this study: - Lule, Skellefte and Dal. Of these three Lule and Skellefte river basins are located in the northern part of Sweden and Dal in the middle. Area, hydropower production and week when spring peak inflow occurs for the three river basins can be seen in Table 1. The different river basins can be seen in Figure 4 and the different measurement stations used as input to the HBV model can be seen in Figure 3.

Table 1 Area, annual average hydropower production and week spring flood peaks based on results for HBV runs for the reference period 1981-2005 for all river basins. Area for Lule and Skellefte received from (vattenmyndigheten.se, n.d. (1)-(2)) and for Dal from (SMHI, 2010).

River basin	Area (km^2)	Hydropower (TWh)	Spring peak inflow (week)
Lule	25 000	13.7	24
Skellefte	12 000	5	21
Dal	29 000	5.5	20

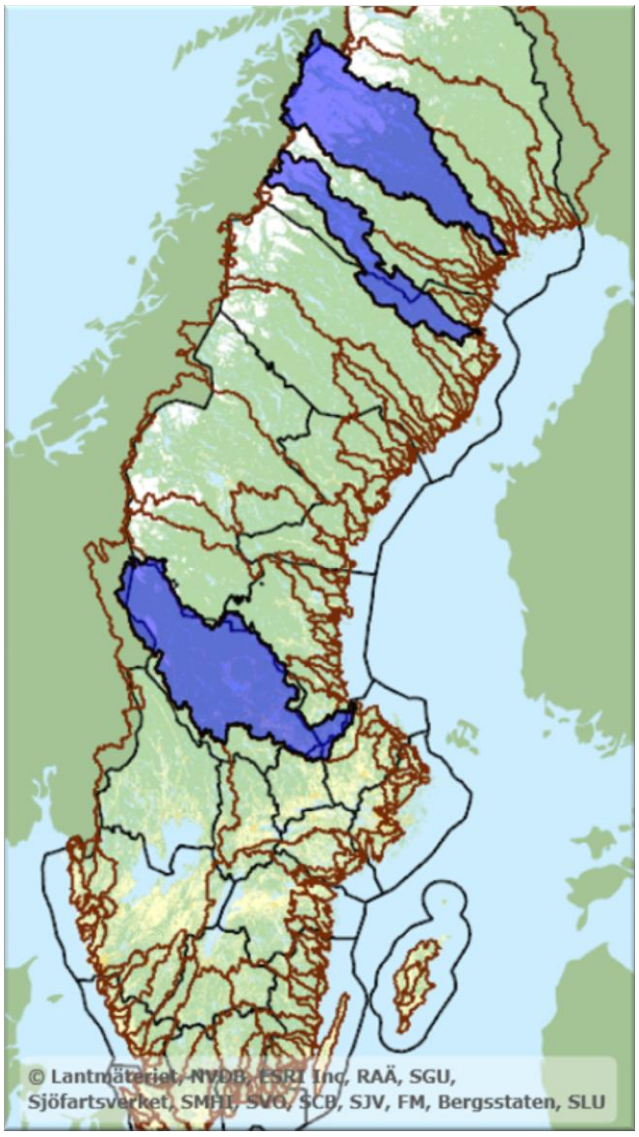

Figure 4 Map from (viss.lansstyrelsen.se, n.d.) showing the three studied river basins.

Figure 3 Map from (maps.google.com, 2012) showing the twelve measurement stations included in the study.

2.3 IPCC

The Intergovernmental Panel on climate Change (IPCC) was established by United Nations Environment programme (UNEP) and the World Meteorological Organization (WMO) in 1988. IPCC is a scientific body working to review and assess the most recent research on climate change and its environmental and socio-economical impacts on the world. Today the organization employs thousands of scientists on a voluntary basis and has 194 member countries. The main objective for IPCC is to provide the world with an up to date, clear and unbiased scientific view on climate change and its impacts (IPCC, n.d).

2.4 Emission scenario

Emission scenarios are estimates of future greenhouse gas emissions that are the basis for the GCM runs. There are several different scenarios depicting different future developments of our civilization. In this project IPCCs A1B scenario was chosen for all runs. The A1 scenario family describes a future with rapid economic growth, rapid introduction of new technologies and a population curve that peaks around 2050 to then start to decline. The A1B scenario in particular is design to depict a future with a balanced mix between fossil and non-fossil fuel sources (IPCC, 2000). The A1B scenario can be seen in Figure 5 as the red dotted line.

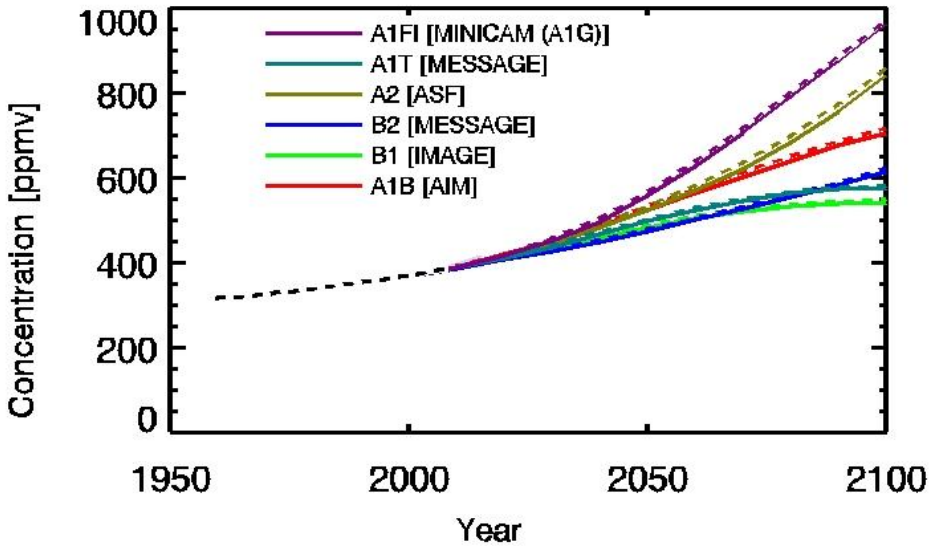

Figure 5 Atmospheric CO_2 concentrations as observed at Mauna Loa from 1958 to 2008 (black dashed line) and projected future CO_2 emissions. A1B, the emission scenario used in this study is the red line in the middle (IPCC, 2011).

2.5 GCM

Global climate models are general circulation models that are based on general principles of fluid- and thermodynamics attempt to describe the complex interaction between the atmosphere, hydrosphere, lithosphere and biosphere (Stute et al. 2011). For this project two different GCMs were chosen, ECHAM5 the 5th generation ECHAM model developed by the Max-Planck institute of meteorology (Max Planck institute of meteorology, 2003), and HADCM3 developed by the Met Office Hadley Centre for Climate Change (Gordon et al., 1999).

2.6 RCM

Regional climate models (RCMs) is a tool for downscaling the output from GCMs to get increased resolution. The higher resolution means more exact representation of surface features such as topography and a more localized description of climate driving processes. Near surface wind speed and precipitation is especially sensitive to horizontal resolution due to their strong interaction with topography and surface physiography (Samuelsson et al., 2010).

In this study result from the Rossby Centre Regional Climate model RCA3 was used for all scenarios.

2.7 HBV model

The HBV model was developed during the 1970s by the Swedish Metrological and Hydrological Institute (SMHI). It is a rainfall-runoff model, which describes the hydrological processes in the basin. Since its development it has been widely used and occurred in research from more than 40 countries (SMHI, 2009). Examples of Swedish studies on water resources that has utilized the HBV model are (Andréasson et al., 2004), (Graham et al., 2007) and (Wetterhall et al., 2011). Andréasson et al., (2004) use the HBV model when they investigated the climate change impacts on six river catchments. Graham et al.,(2007) used the HBV when investigating how the choice of RCM affected the end result of hydrological change. Wetterhall et al., (2011) used the HBV model when they investigated climate changes effect on three river basins in Sweden.

The HBV model is driven by daily observed values of temperature and precipitation. Three important basic sub routines are used and they represent snow melt, soil moisture and runoff (SMHI, 2009). The snowmelt routine in the basic HBV is a degree-day approach. A specific temperature is set in the model and if the temperature is below, precipitation will fall as snow and the runoff will be delayed. The soil routine assumes a statistical distribution of storage capacities in the catchment; the routine is the dominant in runoff formation. The runoff routine transforms the water in the soil and snowmelt routine to runoff and it also add the precipitation that falls on lakes and rivers to get the total runoff (SMHI 2009). The basic structure of the HBV model can be seen in Figure 6.

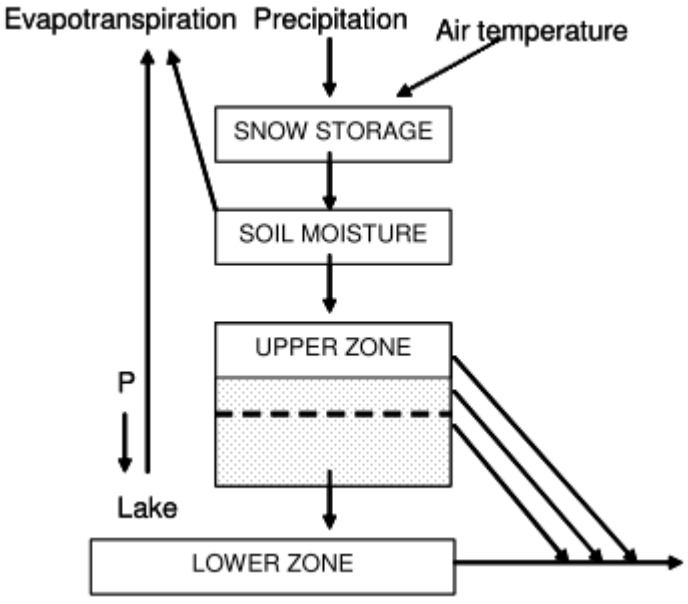

Figure 6 Structure of the HBV model (Lawrence et. al., 2009)

There is no linear transfer function between Increase in precipitation and increased hydropower potential. This is due to the fact that different catchments have different

elevation profiles and hence the amounts of potential energy stored in the water are different (Graham et. al., 2007). The Thomson Reuters Point Carbon HBV model for Sweden estimates inflow directly in energy units (GWh).

3 Problem

3.1 Evaluating bias correction methods

Several reports have investigated the difference in performance of different bias correction methods and evaluated their strengths and weaknesses ((Yang et.al, 2010), (van Roosmalen et.al, 2011) and (Madsen et.al 2010)).

Yang et.al (2010) investigated if the use of a Distribution Based Scaling (DBS) method would improve the results compared to Delta Change (DC) method when transferring RCM data to hydrological model. In the study they found that both methods indicated a warmer and wetter climate. It was concluded that the strength of a DBS approach was that change in future climate variability was included, as opposed to the DC approach where the same variability as in observed data is carried over into modelled future. Yang et al. (2010) also note that DBS will benefit from future development of climate models.

Van Roosmalen et.al (2011) compared a type of DC, and a kind of distribution based scaling. They wanted to investigate if the choice of method would affect the results from the hydrological model. Both correction methods indicated increased flow, DBS some percent higher than DC. The conclusions made in the study were that the choice of method did not affect the mean result. They did not analyse the extreme events so more analysis is needed to investigate if extremes are affected by the choice of methods.

Madsen et.al (2010) used three types of bias correction methods in a study where they examined the climate change effects on hydrology in Sealand, Denmark. The included methods were mean value correction and mean value and variance correction. The result showed that the mean and variance correction method is better at representing the extreme events compared to the mean value correction method. The two methods had similar representation of total mean values and another conclusion by Madsen et al. (2010) was that the mean value correction method should be used if the overall water balance is of interest due to its simplicity.

3.2 Hydrological situation due to climate change in Sweden

Climate change effects on hydrology have plenty of applications such as flood control, city planning and hydropower, and have therefore been the target of several earlier studies.

One such study was made by Graham et al. (2007). Using an ensemble of seven RCMs, two GCMs, varying resolution and two different correction methods the impacts on hydrology in northern Europe was studied with focus on how choice of RCM affected the end result. The average increase in discharge from Lule River for the time period 2071-2100 was 26% for the DBS and 34% for the DC method. The simulations for both bias

correction methods indicated earlier spring floods, the delta change resulted in lower spring peak flows and the DBS slightly higher spring peak flows compared to present conditions. The choice of RCM, GCM and emission scenario had a big impact on the end result for mean runoff in Lule river basin giving a range of runoff increase between 18 to 59 %.

Another study was made by Andréasson et al. (2004) where climate change impacts on hydrology was studied for six Swedish river basins using different climate models, grid resolutions and a DC method. The result showed an increase in annual runoff between 10-35 % in the middle to northern parts of Sweden and a slight decrease in the southern parts. The simulations also showed an increase in precipitation during winter and autumn and a decrease during summer with a decrease in spring flood peaks.

4 Methodology

The reference period for the study is 1981-2005 and it is also the time period the Thomson Reuters point carbon energy model is built around. This is the reason why a 25 year period is studied instead a 30 year period, which is more common in similar research. Observed data was provided by Thomson Reuters Point Carbon.

The resolution for the climate model runs was 50km^2 for HADCM3 and 25 km^2 for ECHAM5. A modified version of the Swedish HBV model developed by Thomson Reuters Point Carbon is used as a hydrological model.

Climate model data for precipitation and temperature for both reference and future periods were provided by Rossby Centre. Modelled gridded data was corrected against observed station data by DHI, and then used as input to the HBV energy model.

A general comment is that the HBV energy model requires a complete time series with all days represented. This poses a problem since the HADCM3 model only has 360 days in one year with 30 days per month. To compensate for this an additional day was added to the HADCM time series for the months with 31 days. The added days had T set to the monthly average and P set to 0. In a similar manner the additional days in February were removed.

The last comment is that all the bias correction methods and DC which are described below, are carried out on output from the climate scenarios for each of the measurement stations.

4.1 Delta change

The delta change approach is an old and often used transfer method (e.g. Bergström et al., 2003, Andréasson et al., 2004 and Graham et al. 2007). In this study a simple version was used where the difference between modelled data for reference and future time period was used to calculate monthly specific climate change factors for temperature, c_T, and precipitation, c_P, (see equation 1-2). The monthly change factors were then applied to the daily observed precipitation and temperature for their respective month to create the future time series (equation 3-4).

$$c_{Tm} = T_{mod,fut} - T_{mod,ref} \quad (1)$$

$$c_{Pm} = \frac{P_{mod,fut}}{P_{mod,ref}} \quad (2)$$

$$T_{predicted,fut} = T_{obs} + c_{Tm} \quad (3)$$

$$P_{predicted,fut} = P_{obs} * c_{Pm} \quad (4)$$

4.2 Mean value correction

The second method is a basic version of bias correction where only the differences in monthly mean values are corrected for. Monthly specific correction factors are calculated both for temperature and precipitation. The correction factor, a, is obtained from the difference between monthly mean values for observed data and modelled data, for the reference period (equation 5-6).

$$a_{Pm} = \frac{P_{obs}}{P_{ref}} \quad (5)$$

$$a_{Tm} = T_{obs} - T_{ref} \quad (6)$$

The monthly correction factors are then applied to the P and T output from the RCM scenario run (modelled future time period) for 2016-2040 and 2076-2100 according to equation 7 and 8.

$$P_{future} = a_{Pm} * P_{scenario} \quad (7)$$

$$T_{future} = T_{scenario} + a_{Tm} \quad (8)$$

4.3 Mean and variance correction

The mean and variance correction method is a further development of the mean value correction method presented above. In this method the difference in variance between observed and modelled precipitation is also corrected for.

The monthly variance is calculated for both observed and modelled data for the reference period. To get equal variance in the observed and the modelled data a correction factor b is introduced (equation 9). The factor b is calculated for each month which means that a total of twelve different b are calculated.

$$P_{obs} = a * P_{mod,ref}^{b} \quad (9)$$

Mean variance for a specific month in observed data is equal the mean variance for the same respective month in the modelled data raised to b. Calculations for b is shown in equation 10.

$$b = \log \frac{mean\ variance\ observed\ month\ x}{mean\ variance\ modelled\ month\ x} \quad (10)$$

When b has been calculated for month x, all days for that that month are corrected with the corresponding factor b, e.g ${P_{Jan1}}^{b}, \ldots\ldots, {P_{Jan31}}^{b}$. Once the variance has been

accounted for the mean value correction factor a, is calculated for each month in the same way as in the mean value correction method (equation 11).

$$a = \frac{P_{obs}}{P_{ref}^{b}} \qquad (11)$$

After a and b has been calculated they are applied on the modelled future precipitation to get corrected future precipitation (equation 12).

$$P_{corr\ future} = a * P_{mod\ future}^{b} \qquad (12)$$

The temperature is calculated the same way as in the mean value correction method.

4.4 Quantile mapping method

The final bias correction method, a Quantile mapping (QM) method, was developed by DHI. Temperature is corrected on a monthly basis as for the previous bias correction methods. This method, however uses a linear regression approach to match the modelled data to the observed data for the reference period, according to equation 13. Two coefficients a_m and b_m are calculated to get the best possible fit between the distribution of observed temperature and RCM output. This is illustrated in Figure 7.

$$T_{corr,ref} = T_{RCM,ref} + a_m + b_m * T_{RCM,ref} \qquad (13)$$

a_m and b_m are then used to correct the future temperature according to equation 14.

$$T_{corr,fut} = T_{RCM,fut} + a_m + b_m * T_{RCM,fut} \qquad (14)$$

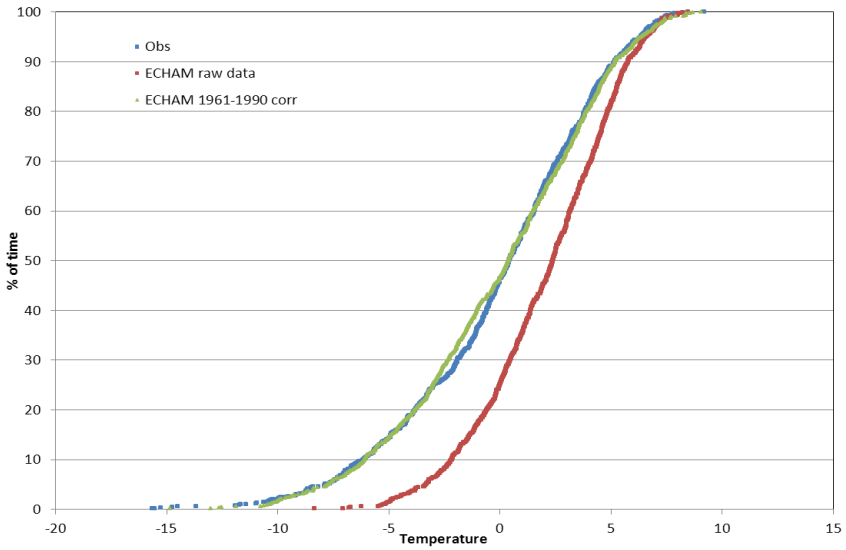

Figure 7: Observed temperature for the reference period (blue line), raw data from climate model for the reference period (red line) and corrected modelled data for the reference period (green line) (DHI, 2011).

For precipitation the first step is to correct the number of wet days which is overestimated by the model. In order to do so precipitation results are sorted from smallest to largest, both for modelled and observed. A cutoff value is determined by taking the corresponding precipitation in modelled results for the percentile where observed precipitation is no longer zero, see Figure 8. All values below this cutoff value

are set to 0 in the modelled data (Figure 9). The correction is made seasonally DJF (Dec-Feb), MAM (Mar-May), JJA (Jun-Aug) and SON (Sep-Nov).

Once the cutoff value has been applied, one correction factor is calculated for each day with precipitation. All correction factors are then divided in two partitions, separated by the 95th percentile, and a polynomial function is fitted to each partition. This can be seen in Figure 10 where the percentiles are plotted against their corresponding correction factors. In this way the correction of normal precipitation and extremes are differentiated.

The cutoff value determined from the modelled reference is then applied to the future modelled results in the same manner with all values below it set to 0. In this way QM has the ability to capture future changes in amount of rainy days. Then, the polynomial functions are applied to the remaining rainfall days.

Date	OBS	Date	RCM 1	Date	RCM 2
23/05/1990	0	12/04/1970	0.77	26/03/1978	0.97
25/05/1990	0	01/04/1973	0.78	28/03/1978	0.97
26/05/1990	0	10/04/1977	0.78	24/04/1964	0.97
29/05/1990	0	06/05/1962	0.78	07/04/1981	0.97
07/03/1962	0.1	15/05/1969	0.79	30/05/1987	0.98
08/03/1965	0.1	07/05/1986	0.79	18/03/1988	0.98
17/03/1966	0.1	31/05/1988	0.79	20/04/1978	0.98
26/03/1967	0.1	03/03/1990	0.8	14/05/1964	0.98
21/03/1971	0.1	03/04/1971	0.8	02/03/1964	0.99
26/03/1971	0.1	10/04/1983	0.8	13/03/1985	0.99
17/03/1975	0.1	18/03/1981	0.81	12/03/1988	0.99
30/03/1975	0.1	28/05/1989	0.81	25/04/1973	0.99
01/03/1976	0.1	28/03/1982	0.82	30/04/1977	0.99
09/03/1976	0.1	27/03/1989	0.82	23/04/1982	1.00
10/03/1976	0.1	05/05/1984	0.82	01/05/1980	1.00
24/03/1976	0.1	29/05/1989	0.82	31/03/1973	1.01
30/03/1976	0.1	22/03/1978	0.83	18/03/1978	1.01

Figure 8: Example explaining the RCM adjustment of spurious drizzle. The cut off value is set to 0.79 for RCM1, all rainfall days ending up below that number are set to 0 as can be seen in Figure 7 (DHI, 2011).

Date	OBS	Date	RCM 1	Date	RCM 2
23/05/1990	0	12/04/1970	0	26/03/1978	0
25/05/1990	0	01/04/1973	0	28/03/1978	0
26/05/1990	0	10/04/1977	0	24/04/1964	0
29/05/1990	0	06/05/1962	0	07/04/1981	0
07/03/1962	0.1	15/05/1969	0.79	30/05/1987	0.98
08/03/1965	0.1	07/05/1986	0.79	18/03/1988	0.98
17/03/1966	0.1	31/05/1988	0.79	20/04/1978	0.98
26/03/1967	0.1	03/03/1990	0.8	14/05/1964	0.98
21/03/1971	0.1	03/04/1971	0.8	02/03/1964	0.99
26/03/1971	0.1	10/04/1983	0.8	13/03/1985	0.99
17/03/1975	0.1	18/03/1981	0.81	12/03/1988	0.99
30/03/1975	0.1	28/05/1989	0.81	25/04/1973	0.99
01/03/1976	0.1	28/03/1982	0.82	30/04/1977	0.99
09/03/1976	0.1	27/03/1989	0.82	23/04/1982	1.00
10/03/1976	0.1	05/05/1984	0.82	01/05/1980	1.00
24/03/1976	0.1	29/05/1989	0.82	31/03/1973	1.01
30/03/1976	0.1	22/03/1978	0.83	18/03/1978	1.01

Figure 9 Continuation of Figure 8where the spurious drizzle has been removed (DHI, 2011).

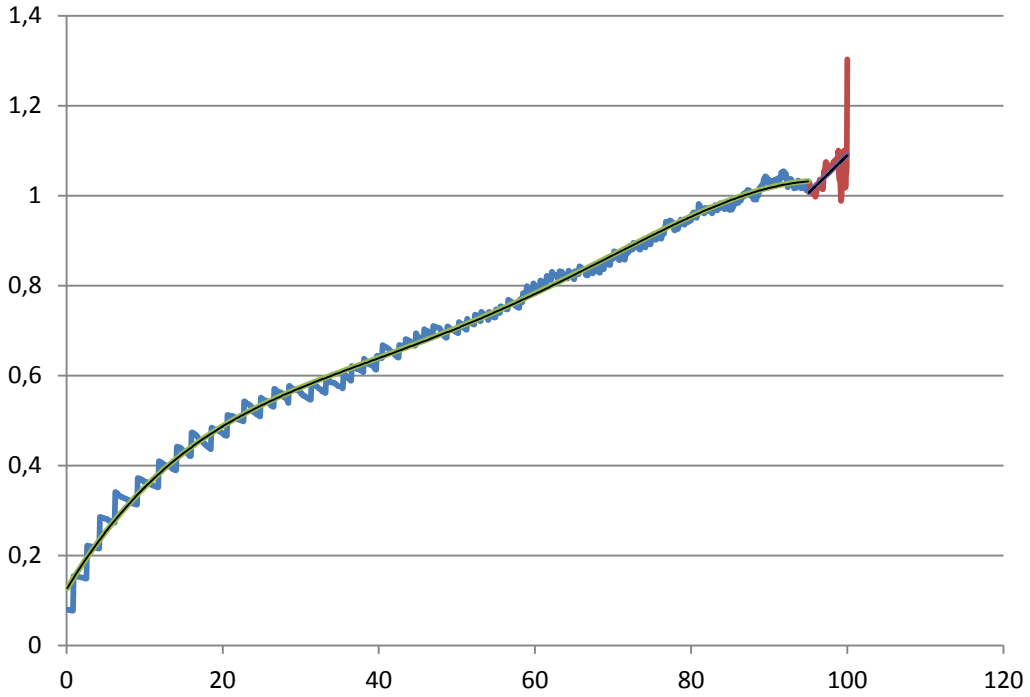

Figure 10: Shows the percentile on the x-axis and the corresponding correction factors on the y-axis. The blue line is corrections factors up to the 95th percentile and the red is up to 100th percentile. The green line is a polynomial used to correct the future modelled data (DHI, 2011).

5 Uncertainties

When interpreting the result from a hydrological model it is important to have a general idea of how big the uncertainties are. Since the model deals with the future there is no "correct answer" to compare the result with. This is why the modelled data is corrected for in different ways by comparing it to earlier time periods where there are observed data available.

All of the bias correction methods in some way use correction factors calculated based on comparisons between modelled and observed data for the reference period. This means it is assumed the systematic bias between modelled and observed will be the same in the future as it is now, which may not be the case (Graham et. al., 2010), (Piani et al., 2010).

Different time periods were used, 2076-2100 for ECHAM5 and 2074-2098 for HADCM3. This was due to an oversight in the beginning of the project of how far the HADLEY model was valid but it is deemed to have only a minor impact on the result. For simplicity the second time period for both ECHAM and HADCM will be referred to as 2076-2100 for the remainder of this study.

6 Results

6.1 Uncorrected data and reason for bias correction

This part serves as an introduction to the results, highlighting the systematic bias in the uncorrected precipitation and temperature from the two climate models.

Figure 11 shows uncorrected precipitation for both ECHAM and HADCM. It can be seen that the modelled data is overestimating the total precipitation by 5-130 % compared to the observed results for the same period.

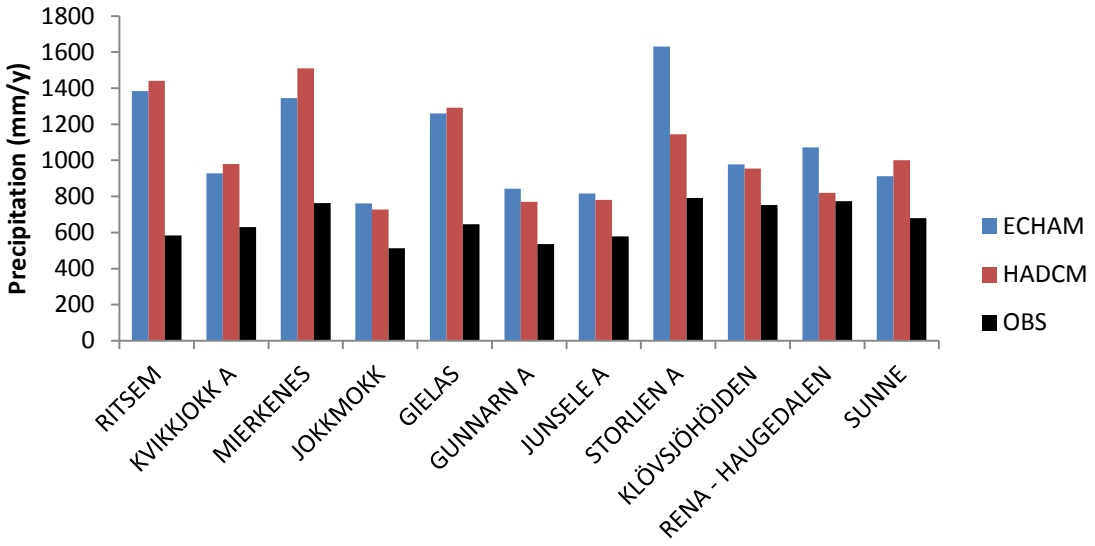

Figure 11 Uncorrected annual mean precipitation for ECHAM and HADCM for reference period compared to observed reference period.

Looking at temperature in Figure 12, ECHAM diverts +/- 0.2 degrees compared to observed, and HADCM consistently underestimates temperature by approximately one degree for most stations. The exception where modelled temperature diverts more from observed is Ritsem and Mierkenes both located at high elevation and altitudes. Similar results were obtained by Van Roosmalen et. al., (2009) that concluded that predicted temperature increase increased with distance from the coast and with higher latitude in Scandinavia.

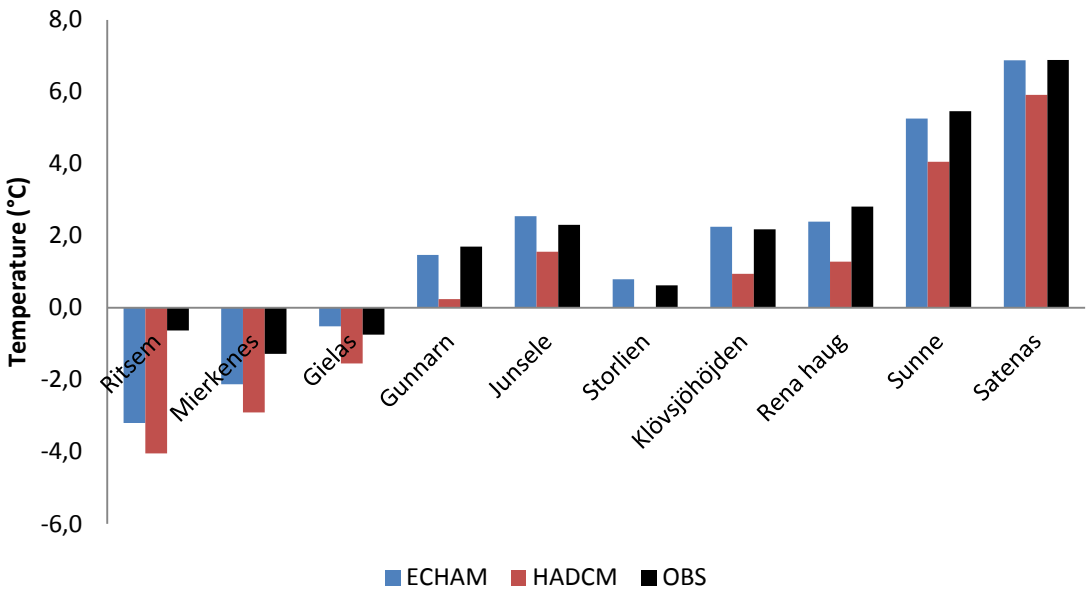

Figure 12 Total average temperature on y-axis for uncorrected ECHAM and HADCM output for reference time period compared to observed results for the reference period.

In Figure 13 the percentage of dry days are plotted for all stations. Observed results shows 40-50 % of dry days whereas modelled results for both ECHAM and HADCM show 5-15 % dry days. The number of days with rain is hence overestimated by about 30-40 % in the modelled results.

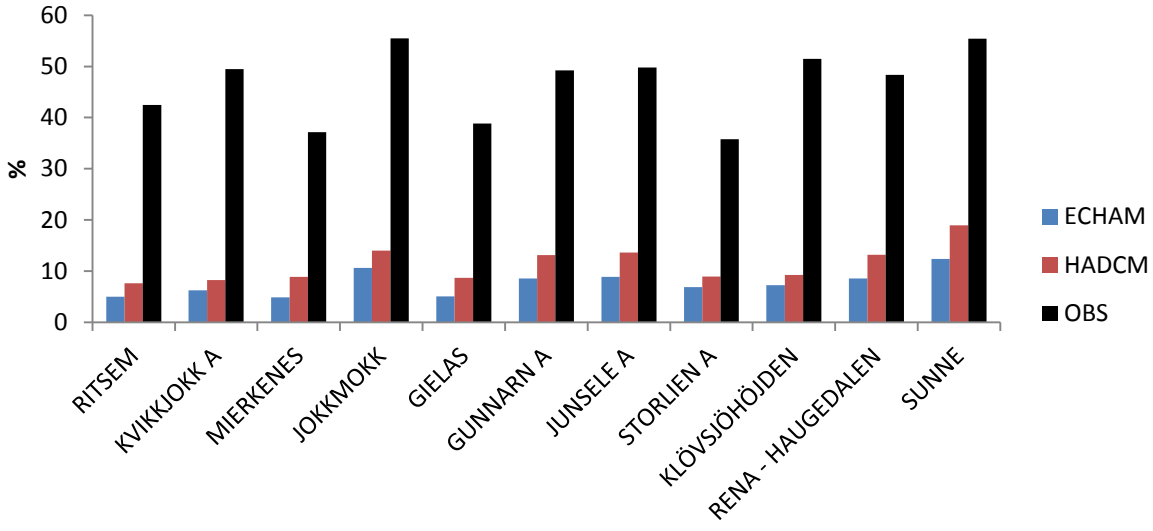

Figure 13 Uncorrected annual percent of dry days for ECHAM and HADCM compared to observed results for the reference period.

6.2 Comparison median and mean values

This section serves to evaluate the impact of looking at mean or median annual results. In Table 3-6 annual mean and median precipitations are compared for all stations and corrections methods.

A general note should be made that for the remainder of this thesis the reference time period is denoted OBS in tables and graphs showing results. This means that even if the caption indicates a different time period for the results, OBS still refers to the observed values for the reference time period 1981-2005.

The ECHAM results for the first time period are presented in Table 3. No clear pattern can be discerned and the overall difference between mean or median results for precipitation is between 0-6 %.

It can be seen in Table 3 that DC and MV mean values are always the same. This is due to the way the two methods correct for precipitation. This can be illustrated by a simple example. Using the values presented in Table 2 in equation 15-16 it can be seen that when calculating any total sum or average for the corrected future DC and MV will give the same result. The difference in hydrological effects is due to different distribution of data within the data series, were DC is based on observed precipitation and MV is based on modelled precipitation. This is the reason why median values for the two methods are different.

Table 2 Example values of total annual observed, modelled reference and modelled future results.

OBS (ref)	Modelled ref	Modelled future
300	400	500

$$DC = \frac{Modelled\ future}{Modelled\ ref} * OBS = \frac{500}{400} * 300 = 375 \quad (15)$$

$$MV = \frac{OBS}{Modelled\ ref} * Modelled\ future = \frac{300}{400} * 500 = 375 \quad (16)$$

Table 3 ECHAM 2016-2040, median and mean average annual precipitation for all bias correction methods and stations.

ECHAM	OBS		DC		MV		MVV		QM	
Station name	median	mean	median	mean	median	mean	median	mean	median	mean
RITSEM	563	584	576	600	608	600	606	590	614	605
KVIKKJOKK A	638	630	640	636	639	636	644	635	649	641
MIERKENES	748	764	758	774	797	774	790	773	794	779
JOKKMOKK	528	514	541	529	519	529	522	528	535	532
GIELAS	649	647	646	641	648	641	644	638	646	638
GUNNARN A	516	537	516	533	527	533	535	534	516	533
JUNSELE A	559	579	556	576	584	576	584	574	580	574
STORLIEN A	808	792	816	795	781	795	792	792	764	797

KLÖVSJÖHÖJDEN	716	752	733	779	756	779	764	788	762	791
RENA - HAUGEDALEN	741	773	735	769	768	769	767	772	789	776
SUNNE	655	679	666	688	692	688	697	692	701	692

Table 4 with results for ECHAM 2076-2100 shows similar results as Table 3. The difference in mean and median precipitation varies between 0-5 %.

Table 4 ECHAM 2076-2100, median and mean average annual precipitation for all bias correction methods and stations.

ECHAM	OBS		DC		MV		MVV		QM	
Station name	median	mean	median	mean	median	mean	median	mean	median	mean
RITSEM	563	584	639	662	660	662	643	642	705	679
KVIKKJOKK A	638	630	763	756	740	756	741	763	739	771
MIERKENES	748	764	822	845	865	845	855	849	878	856
JOKKMOKK	528	514	634	618	620	618	623	621	619	626
GIELAS	649	647	719	723	720	723	713	720	722	722
GUNNARN A	516	537	595	621	621	621	617	620	624	628
JUNSELE A	559	579	647	671	679	671	683	669	670	677
STORLIEN A	808	792	860	830	840	830	837	824	829	831
KLÖVSJÖHÖJDEN	716	752	820	858	860	858	883	872	863	874
RENA - HAUGEDALEN	741	773	838	864	857	864	859	868	883	875
SUNNE	655	679	720	747	732	747	732	748	748	762

Table 5 presents the HADCM 2016-2040 difference between annual median and mean precipitation. Results are similar to those for ECHAM apart from the precipitation estimates being higher. Difference between annual median and mean is 0-5 %.

Table 5 HADCM 2016-2040, median and mean average annual precipitation for all bias correction methods and stations.

HADCM	OBS		DC		MV		MVV		QM	
Station name	median	mean	median	mean	median	mean	median	mean	median	mean
RITSEM	563	584	633	668	648	665	631	653	672	655
KVIKKJOKK A	638	630	751	737	739	736	755	751	734	722
MIERKENES	748	764	858	874	833	871	830	866	815	860
JOKKMOKK	528	514	629	619	624	618	637	637	605	597
GIELAS	649	647	731	742	735	740	712	731	712	731
GUNNARN A	516	537	586	608	593	607	610	609	585	594
JUNSELE A	559	579	631	650	643	649	636	649	632	643
STORLIEN A	808	792	898	870	865	867	868	872	863	862
KLÖVSJÖHÖJDEN	716	752	824	849	849	848	854	861	848	842
RENA - HAUGEDALEN	741	773	846	872	864	871	866	894	864	865
SUNNE	655	679	738	759	763	758	766	760	728	740

In Table 6 HADCM results for the second time period is presented. The difference between mean and median precipitation is approximately the same as in Table 3-5, 0-5 %.

Table 6 HADCM 2076-2100, median and mean average annual precipitation for all bias correction methods and stations.

HADCM	OBS		DC		MV		MVV		QM	
Station name	median	mean	median	mean	median	mean	median	mean	median	mean
RITSEM	563	584	683	715	723	712	711	691	724	707
KVIKKJOKK A	638	630	835	822	831	819	836	837	803	817
MIERKENES	748	764	913	927	944	924	929	915	925	900
JOKKMOKK	528	514	695	683	697	680	692	688	675	668
GIELAS	649	647	781	801	818	798	801	779	802	785
GUNNARN A	516	537	686	717	702	715	705	715	710	708
JUNSELE A	559	579	733	758	753	756	742	748	739	760
STORLIEN A	808	792	982	934	945	930	951	938	953	935
KLÖVSJÖHÖJDEN	716	752	903	947	958	945	970	973	969	968
RENA - HAUGEDALEN	741	773	939	969	962	967	982	1003	962	976
SUNNE	655	679	779	797	792	794	799	791	797	794

Overall the difference between annual mean and median precipitation are approximately the same, 0-6 %, regardless of time period or GCM. The observed difference between mean and median precipitation varies in the same region as the modelled precipitation, between 0-5 %. DC is the correction method that often shows the highest difference between mean and median precipitation for both ECHAM and HADCM. MV and MVV are the two that have the smallest difference between mean and median precipitation.

Since no clear patterns could be discerned and difference between mean or median values was small, a decision was made to only study mean values for the remainder of the project. Mean was chosen since it is most common in similar research and best represents total change for the hydropower application.

6.2.1 Change in precipitation

In this section (Figure 14-16) the change in total precipitation compared to observed is calculated based on mean results in Table 3-6.

Figure 14 shows ECHAM 2016-2040 results and the change in total precipitation ranges from a decrease with 1.2 percent to an increase with 5.1 percent. QM is the correction method that indicates the biggest change overall.

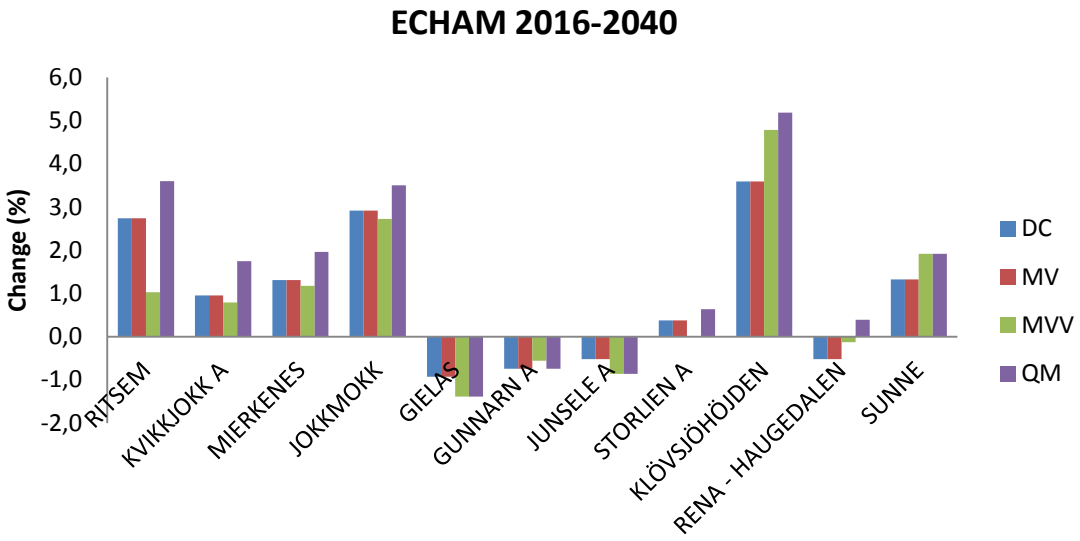

Figure 14 ECHAM 2016-2040 change of total precipitation compared with observed precipitation for all stations.

ECHAM results for the second time period show an increase between 4-22 % and as for Figure 14, QM indicate the highest increase.

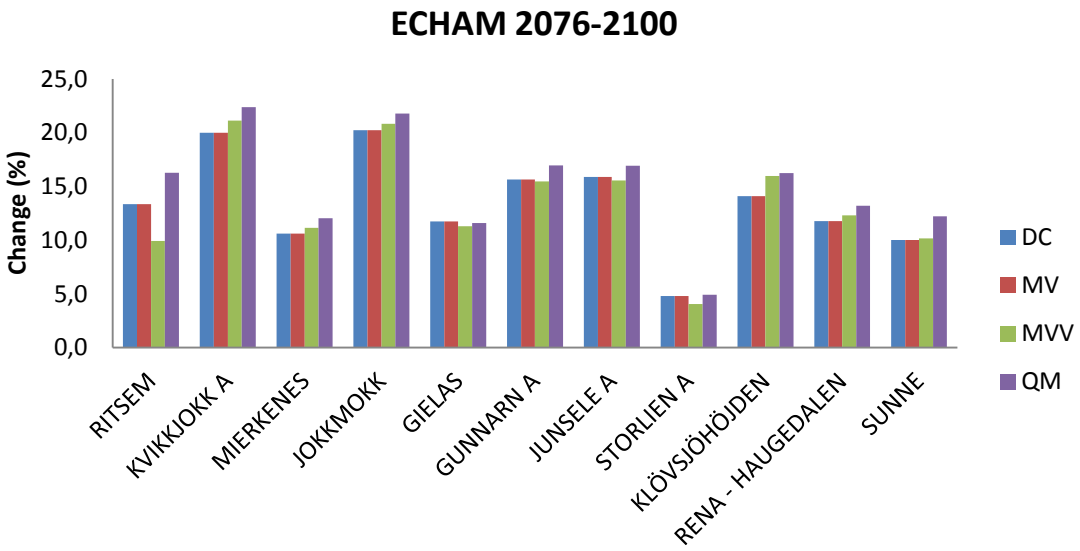

Figure 15 ECHAM 2076-2100 change of total precipitation compared with observed precipitation for all stations.

Figure 16 presents the change in precipitation generated by HADCM for all stations during the first time period. The overall increase is between 9-24 %. MVV indicate the highest precipitation increase compared to observed precipitation.

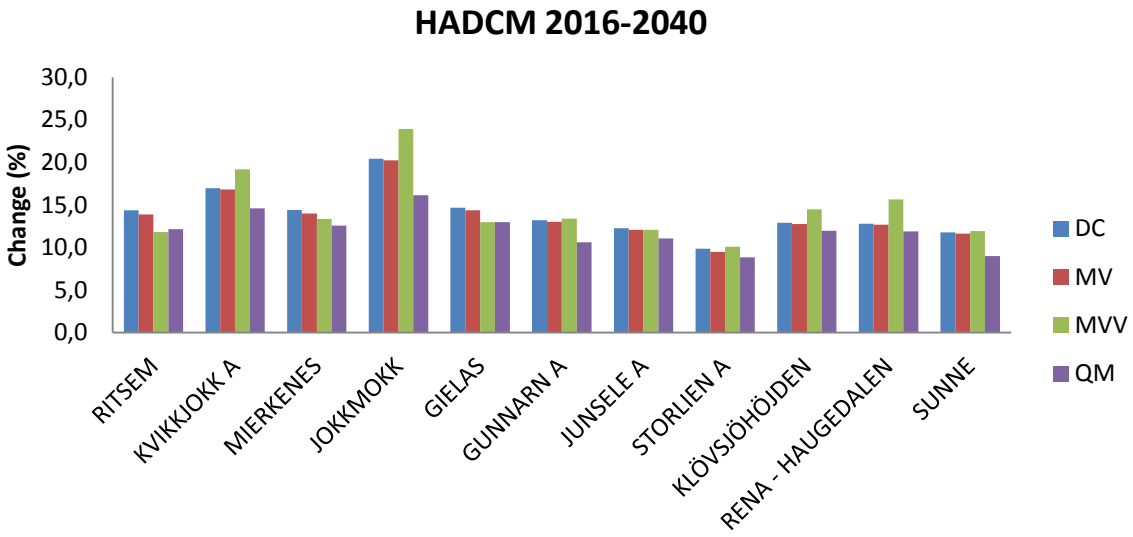

Figure 16 HADCM 2016-2040 change of total precipitation compared with observed precipitation for all stations.

During the second time period HADCM results show an increase with between 16-34 % (Figure 17). No correction method stands out in any particular way.

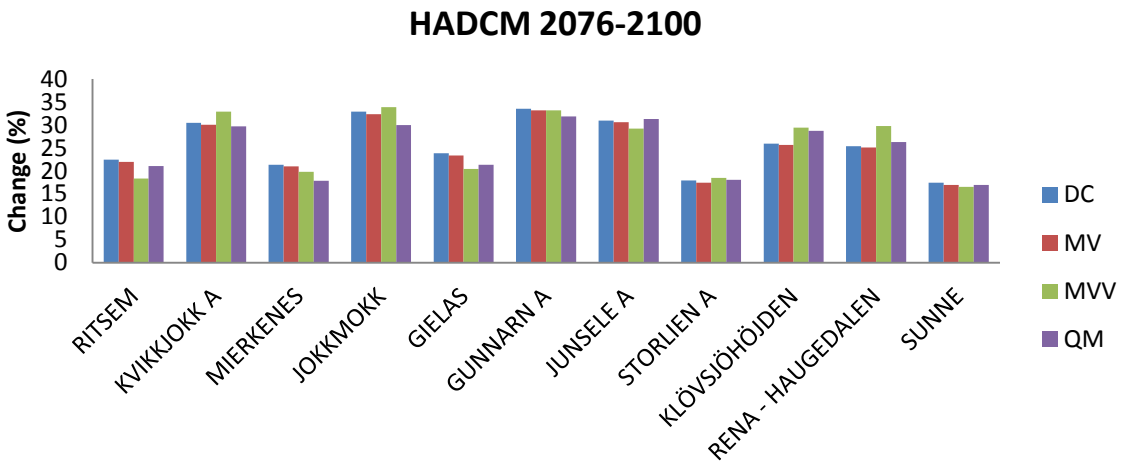

Figure 17 HADCM 2076-2100 change of total precipitation compared to observed precipitation for all stations.

During the first time period, ECHAM change varies between -1 to +5 % with a mean change for all stations and correction methods of 1.1. HADCM results for the same time period shows an increase of 9-24 with a mean of 13.5 %.

For the second time period ECHAM indicates an increase of 4-22 % compared to the HADCM that show an increase of 16-34%. The average increase for ECHAM it is 13.8 % and for HADCM 25.3 %. Overall HADCM results show an increase that is 12 points higher than that of ECHAM for both time periods.

For ECHAM it is QM that indicates the highest increase in total precipitation and for HADCM it is MVV, for the majority of the stations.

DC and MV should as was earlier concluded always show the same increase for total mean based on how the methods correct for bias. For some stations however the HADCM results a differ one percent between DC and MV. This is most likely a result of how the leap year day was corrected for in the HADCM data to get a complete time series for the hydrological model. This could be considered as a calculation error, but it is judged little impact on the total result.

6.2.2 Average monthly precipitation for three stations

This section serves to evaluate the monthly average and monthly change in precipitation compared to observed. In Table 7-9 the results of the correction methods are presented for the second time period 2076-2100 for both ECHAM and HADCM. Only three out of the twelve stations were included to avoid having to many tables. Ritsem, Junsele and Sunne were chosen since they represent the north, middle and south respectively.

6.2.2.1 Ritsem

Ritsem is the most northern station and in Table 7**Error! Reference source not found.** the monthly average precipitation and the change compared to observe precipitation can be seen.

For ECHAM the highest percentage increase in precipitation occurs during spring and early summer, April-June. The increase varies from 7-79 %. The highest amount of precipitation falls during July-September, 65-81 millimeters. QM is the correction method that indicates the biggest changes both for increase and decrease. The interval for the change indicated by QM is a decrease with 30 to an increase with 79 %.

For HADCM there are two periods that have high percentage increase and they are April-May and October-December. The precipitation increase in these two periods is 0-79 %. The most precipitation comes during the months July-January and the amount varies from 44-85 millimeters.

Table 7 Ritsem monthly average precipitation and change in precipitation for all bias correction methods and both GCMs for the second time period 2076-2100.

Ritsem	Mean	Change	Mean	Change	Mean	Change	Mean	Change
Month	E-DC		E-MV		E-MVV		E-QM	
J	60	-5	60	-5	60	-4	50	-20
F	46	5	46	5	46	4	42	-4
M	37	6	37	6	38	7	25	-30
A	30	24	30	24	26	7	32	31
M	41	33	41	33	37	19	54	76
J	56	51	56	51	52	40	67	79
J	82	13	82	13	81	12	73	1
A	72	11	72	11	71	10	84	30
S	65	21	65	21	62	15	81	50
O	64	14	64	14	63	11	63	12
N	48	10	48	10	46	7	37	-14
D	60	2	60	2	60	2	69	18
Month	H-DC		H-MV		H-MVV		H-QM	

J	82	31	82	31	85	35	71	13
F	47	6	44	0	44	-1	60	36
M	40	14	40	14	38	8	28	-20
A	30	23	30	23	26	9	31	30
M	41	33	41	33	37	18	55	79
J	43	15	43	15	41	10	51	38
J	84	17	84	17	82	13	68	-6
A	68	6	68	6	66	2	79	23
S	51	-6	51	-6	52	-4	79	46
O	85	51	85	51	82	45	68	21
N	64	46	64	46	60	38	44	0
D	79	36	79	36	80	36	71	21

6.2.2.2 Junsele

In Junsele the months with the highest increase for ECHAM precipitation are January-Mars and May-June, see Table 8. The increase varies from 11-35 %. The period during the year with the most precipitation is summer June-August, during this period the precipitation varies from 72-108 millimetres.

For HADCM precipitation there is a general increase with over 22 %, the months that diverts from the high increase are Mars and August. During these two months change varies from -5 to +17 %.

Table 8 Junsele, monthly average precipitation and change in precipitation for all bias correction methods and both GCMs for the second time period 2076-2100.

Junsele	Mean	Change	Mean	Change	Mean	Change	Mean	Change
Month	E-DC		E-MV		E-MVV		E-QM	
J	55	31	55	31	56	32	46	11
F	32	19	32	19	31	15	36	34
M	37	23	37	23	36	20	37	25
A	31	0	31	0	31	2	33	7
M	50	28	50	28	51	30	53	35
J	72	22	72	22	73	23	77	31
J	107	26	107	26	108	27	93	10
A	73	-4	73	-4	73	-4	79	3
S	56	4	56	4	56	3	62	14
O	54	10	54	10	54	10	58	19
N	54	17	54	17	53	15	47	3
D	48	17	48	17	48	17	55	34
Month	H-DC		H-MV		H-MVV		H-QM	
J	61	45	61	45	61	45	53	26
F	36	33	34	26	31	15	43	59

M	34	13	34	13	33	10	35	17
A	40	29	40	29	40	29	35	13
M	57	46	57	46	55	41	63	62
J	80	36	80	36	78	32	88	49
J	132	55	132	55	132	55	111	31
A	72	-5	72	-5	72	-5	80	5
S	60	11	60	11	59	9	75	39
O	71	45	71	45	71	45	59	20
N	59	28	59	28	56	22	59	28
D	56	37	56	37	58	41	58	41

6.2.2.3 Sunne

For Sunne the months with the biggest precipitation increase for ECHAM are January-February and October-November, see Table 9. During these months the increase is 18-46 % compared to observed precipitation. It is during summer and autumn months that most of the precipitation comes. The precipitation during these months is between 63-85 millimeters.

May and November-December are the months with the overall highest precipitation increase, varying between 23-45 %. During summer and autumn the monthly average are at their highest. The precipitation during these months is 67-100 millimeters.

Table 9 Sunne monthly average precipitation and change in precipitation for all bias correction methods and both GCMs for the second time period 2076-2100.

Sunne	Mean	Change	Mean	Change	Mean	Change	Mean	Change
Month	E-DC		E-MV		E-MVV		E-QM	
J	62	46	62	46	62	45	61	43
F	39	19	39	19	38	17	44	36
M	37	6	37	6	38	9	43	24
A	51	21	51	21	52	24	39	-8
M	52	6	52	6	52	6	59	19
J	79	3	79	3	80	3	64	-17
J	73	-3	73	-3	73	-3	85	12
A	79	0	79	0	79	0	85	8
S	63	-7	63	-7	63	-7	69	3
O	83	19	83	19	84	20	82	18
N	76	24	76	24	77	25	75	22
D	51	8	51	8	50	6	55	17
Month	H-DC		H-MV		H-MVV		H-QM	
J	49	14	49	14	48	12	44	3
F	39	20	36	13	35	8	46	43
M	34	-2	34	-2	34	-1	36	4
A	52	24	52	24	52	24	41	-2

M	64	29	64	29	63	28	72	45
J	99	28	99	28	100	29	79	3
J	84	12	84	12	84	12	88	17
A	75	-5	75	-5	75	-5	90	15
S	67	-1	67	-1	67	-1	85	25
O	92	32	92	32	95	36	73	5
N	76	24	76	24	76	23	77	26
D	64	37	64	37	61	31	61	29

6.2.2.4 Summary

Looking at the results for annual mean precipitation DC and MV follow each other as usual. February is the only month there they do not have the same results and it is most likely due to how the leap year was corrected.

HADCM precipitation results indicate a decrease of one to six % for DC, MV and MVV either in September or August. For all stations the majority of precipitation falls during summer.

QM is the methods that have the biggest change interval from -30 to +79 %; the other correction methods show intervals from -7 to +55 %. It would seem that QM is more sensitive which is reasonable to assume considering the way QM corrects small and big rain events differently, see Figure 10. MV, MVV and DC apply the same correction factors to all precipitation. It is interesting to see that it is not QM that indicates the highest increase percent during the month with most precipitation.

6.3 Percent of dry days

This part shows how the different climate models differ in amount of dry days (precipitation = 0). Since the results of this analysis were similar for all stations, only results for Junsele were included in the report to avoid having too many graphs. In this section, the observed data was not included since it exactly corresponds to the amount of dry days in the delta change method.

As can be seen in Figure 18-18, the difference between the numbers of days without precipitation varies greatly between the different methods. The first observation is that DC presents the same number of dry days both time periods. This is as expected considering different change factors for the two time periods are applied to the same data, meaning the amount of dry days can never change in the future compared to the observed.

Mean value and mean value variance results overlap each other for the same time period, but still differ in amount of rainy days between the time periods. This shows how both MV and MVV have the ability to capture future changes in the amount of dry days. The fact that MV and MVV results follow each other in this part for the same time period is expected since the difference between the methods is an added factor in mean value variance that can affect the amount of precipitation, but never make an individual event go down to zero.

The last method is the quantile mapping method, which shows two distinctly different results for the two time periods. This shows how QM just as MV and MVV also has the ability to capture future variability in amount of rainy days. The method by which this is achieved though is very different in QM compared to MV and MVV and the effect of the cutoff value becomes clear. QM results indicate 40-60 % dry days in the future whereas MV and MVV indicate 5-25 %. Compared to the observed / DC results of 40-60 % QM performs closer to what might be expected to be a reasonable result.

Coupled with earlier uncorrected GCM results seen in Figure 13 which display the exact same underestimation in amount of dry days it becomes clear this is a systematic bias that MV and MVV simply doesn't correct for.

A note should be made that since these models are predictions of the future it is impossible to exclude the possibility that the amount of rainy days might in fact change as drastically as MV and MVV predicts. It would however seem highly unlikely.

In general all three methods MV, MVV and QM indicate a decrease in the amount of dry days from the first to the second time period. QM indicates the biggest change between 5-15 %. MV and MVV show very similar results for both ECHAM and HADCM whereas QM give 5-10 % lower predictions in amount of dry days for the first time period in HADCM compared to ECHAM. For the second time period QM results convene for both GCMs.

QM show a similar pattern in how the amount of dry days is distributed over the year compared to observed results. Since QM uses a cutoff value this would mean that the increase in amount of rainfall events over a certain size is relatively evenly distributed over the year.

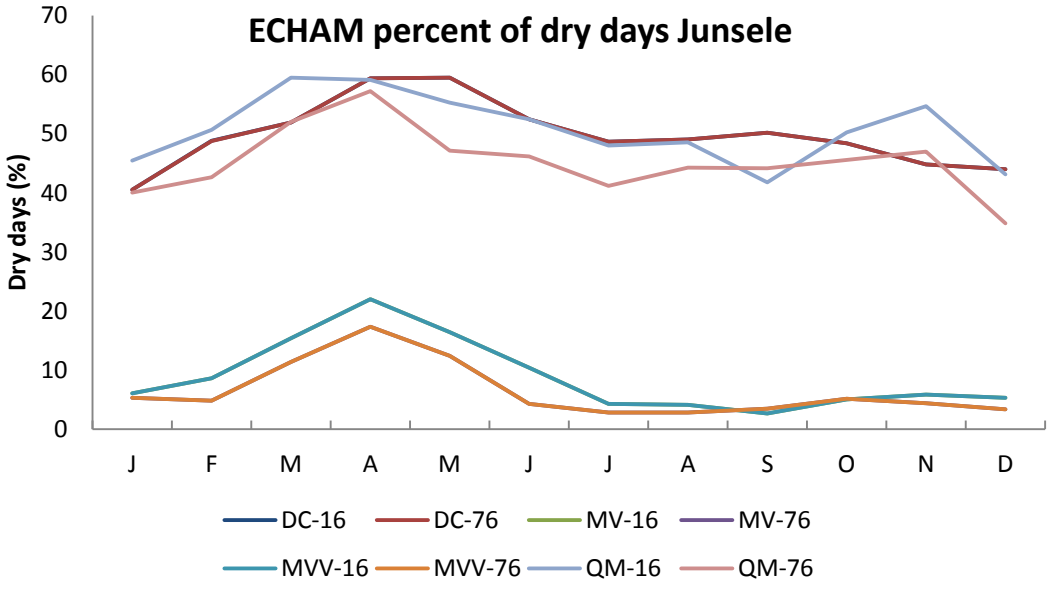

Figure 18 Junsele, ECHAM percent dry days on y-axis and Jan-Dec on x-axis.

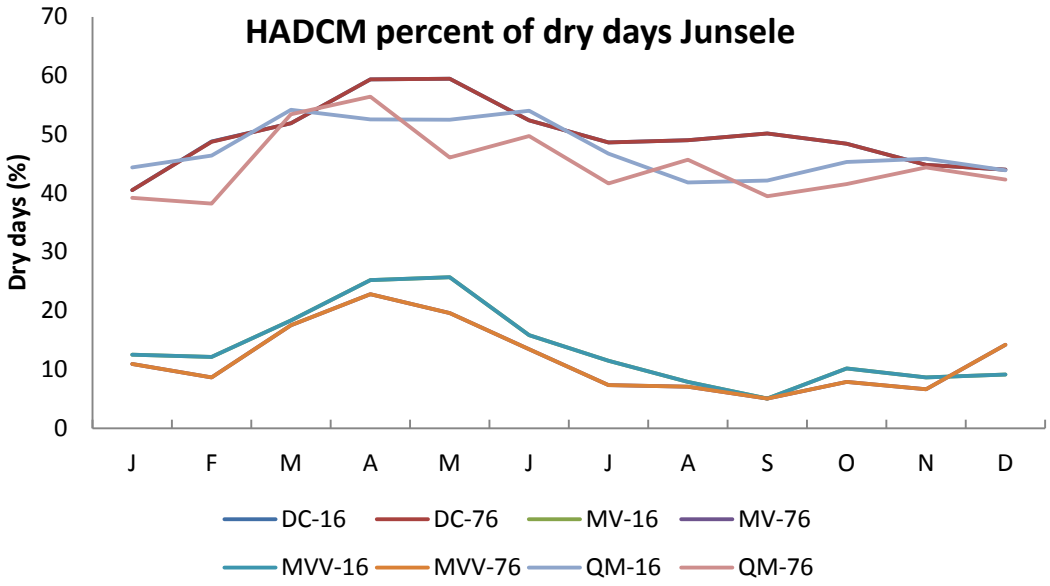

Figure 19 Junsele, HADCM percent dry days on y-axis and Jan-Dec on x-axis.

Table 10 presents results on how much precipitation that can be found within the percent difference in the amount of dry days in MV and MVV compared to observed. HADCM results show 3-6 % of the total precipitation and EHCAM show 5-8. This says something about the size of the different rainfall events that are present in the MV and MVV results. Since MV and MVV have on average 30 % more days with rain compared to observed and QM and still only 3-8 % of the total precipitation is present in those 30 %, the rain events must me quite small.

Table 10 Percent of total precipitation that is contained within the overestimated percentiles in MV, calculated as the percent of precipitation making up the difference in amount of dry days between MV and QM.

	Ritsem	Junsele	Sunne
HADCM	6,7	3,1	4,1
ECHAM	8,4	5,2	5,3

6.4 Extreme events

This section serves to evaluate how the different bias correction methods differ in the way they capture extreme events. In Table 11 and Table 12 the average of the top five extremes for the entire time period is presented for both ECHAM and HADCM.

MV and MVV show the lowest results for ECHAM extreme events for both time periods for all three measurement stations. The pattern is most pronounced for Ritsem where the top five extreme events for both MV and MVV hold less than 50 % of the precipitation of both DC, QM and observed.

That MV and MVV have lower extreme events is not entirely surprising based on earlier results e.g. Figure 18 with regards to amount of dry days. It has been concluded both

methods have an overrepresentation in the amount of wet days. Since the total mean for the entire year is the same for both DC and MV, the 3-8 % precipitation that was present in the additional days with rain present in the MV and MVV results compared to QM and observed has to have diminished the rest of the precipitation events by as much.

Overall the ECHAM results indicate no sign of increase of the most extreme events in the future.

Table 11 Average of the top five extreme precipitation events for three stations compared to observed results.

ECHAM	Ritsem (mm)	Junsele (mm)	Sunne (mm)
OBS	45	38	51
DC-16	42	36	52
DC-76	49	40	52
MV-16	21	28	32
MV-76	19	29	37
MVV-16	17	29	42
MVV-76	16	32	42
QM-16	44	40	51
QM-76	43	41	60

Compared to ECHAM the HADCM results in Table 12 differ in many ways. Overall values are higher, for Junsele every bias correction method for both time periods show an increase compared to observed where for ECHAM it was only three out of eight. There is also an overall pattern of increase in extreme events from the first to the second time period. Lastly the total highest extreme event for HADCM is 11 mm higher than the highest extreme event for ECHAM.

MV and MVV results for Ritsem and Sunne are lower than for QM and DC as was the case for ECHAM. For Junsele however the pattern has changed and MV and MVV give higher results than DC and almost as high as QM.

Overall QM gives the highest results for both ECHAM and HADCM. This could be explained both by the fact that QM applies one correction factor for each percentile and that it uses a separate polynomial fit for the top five percent.

Table 12 Average of the top five extreme precipitation events for three stations are compared to observed extremes.

HADCM	Ritsem(mm)	Junsele(mm)	Sunne(mm)
OBS	45	38	51
DC-16	52	41	52
DC-76	52	45	52
MV-16	23	45	35
MV-76	27	49	37
MVV-16	24	46	40

MVV-76	26	50	41
QM-16	44	45	62
QM-76	52	53	71

6.5 Temperature

Temperature is calculated the exact same way for the MV and MVV methods and is therefore represented with the acronym MEAN. Since the temperature in Figure 20 is seen as average temperatures for the entire period the delta change method also gets the exact same values as the mean variance method. There is however a difference in the distribution of daily temperatures within the data between the DC and the MV and MVV, which cannot be seen in this picture. QM show consistently 0.1-0.2 degrees higher results compared to MV/DC for ECHAM and -0.1 - +0.3 for HADCM. In general the three bias correction methods show similar results and the major difference is due to choice of GCM. In all figures during this part E stands for ECHAM and H for HADCM.

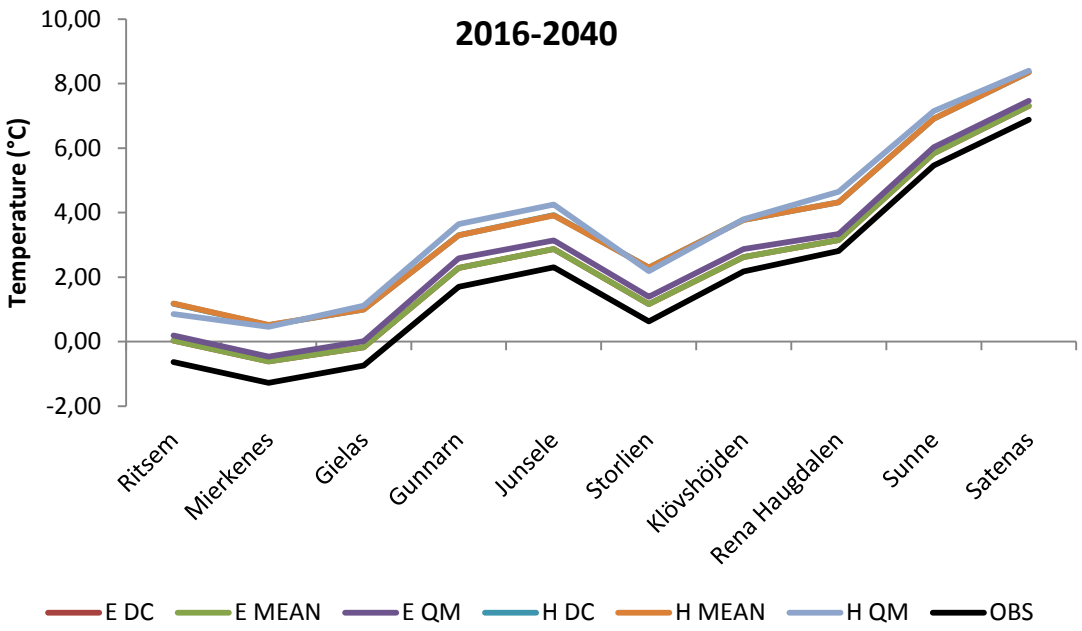

Figure 20 Average temperature for the entire time period 2016-2040 on y-axis.

For the second time period the change in temperature has become bigger and the difference between the different bias correction methods more pronounced, see Figure 21. DC and MV still show the exact same result and show a difference of about one degree between the two global climate models. The QM results are quite interesting and stand out from the other methods. Whereas DC, MV and MVV results differ mainly due to which GCM is used, QM have similar results for both GCMs during the second time period. This means that for example ECHAM QM results show temperatures that are 0.2-2.0 degrees higher compared to ECHAM results for the other methods. It would appear that the more advanced way of correcting for temperature bias on the QM method has a clear impact on the end result.

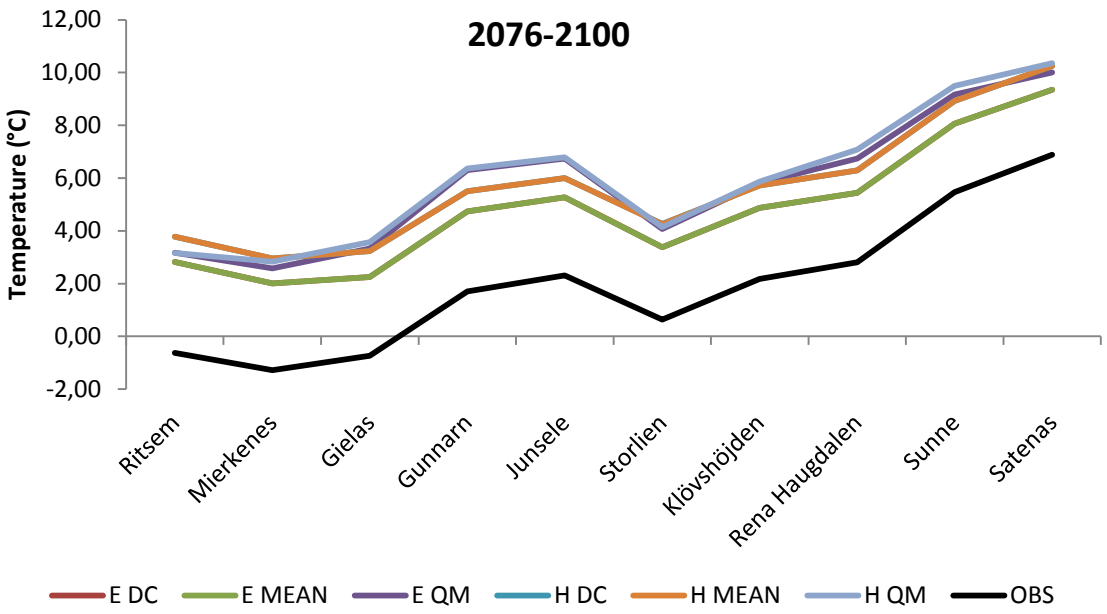

Figure 21 Average temperature for the entire time period 2076-2100 on y-axis. Measurement stations on x-axis.

Looking at Figure 22 and the latitudal distribution of the change in temperature, the slope of all trend lines is positive. This would suggest a pattern between the 58th and the 67th latitude where temperature increase is bigger the further north the station is located.

For the first time period the ECHAM results show an increase in temperature between 0.5-0.7 degrees for DC/MV and 0.7-0.9 degrees for QM. For HADCM the results show an increase of 1.5-1.8 degrees for DC/MV and 1.5-2 degrees for QM.

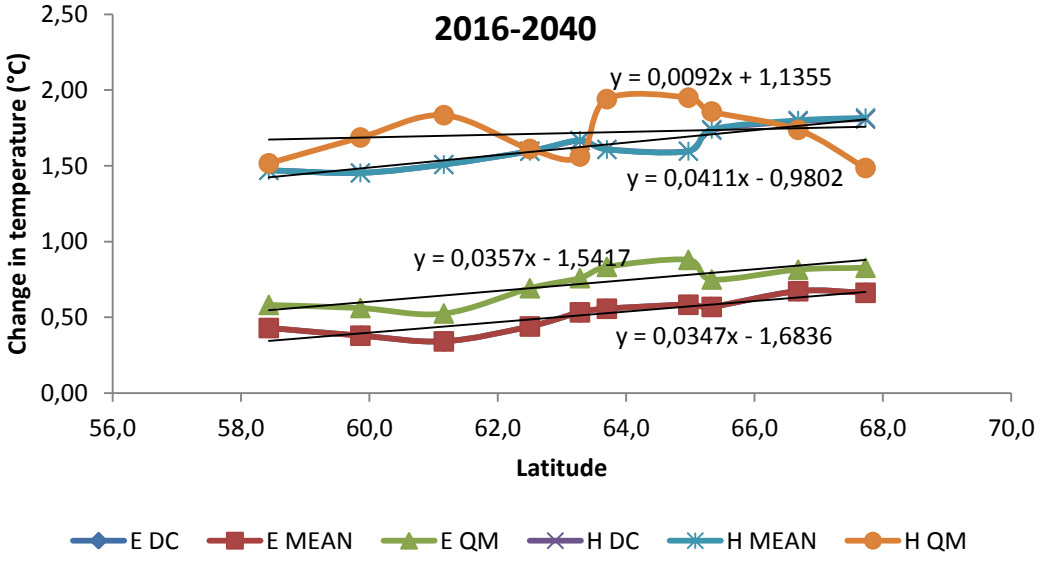

Figure 22 Change in temperature (y-axis) and measurement station latitude (x-axis) for the time period 2016-2040.

For the second time period (Figure 23) the slope of the trend lines are all still positive. This would indicate a higher increase in temperature with higher latitude is still present, at the same time the QM results for both GCMs have very bad R^2 values which would indicate only 10-24 % of the slope in the trend line could be explained by latitude. Six out of eight methods still show very good R^2 values and indicate as in Figure 22 that between the 58th and 67th latitude temperature increase is bigger the further north the station is located.

During the second time period ECHAM results indicate a temperature increase with 2-3.5 °C according to DC MV and MVV results and 3.2-4.6 °C according to QM. This means QM gives an estimate of temperature that is over one degree higher than the three other methods. For HADCM the increase is 3.5-4.5 °C according to DC, MV and MVV results and 3.5-4.7 °C according to QM. HADCM results show much smaller differences between the different correction methods.

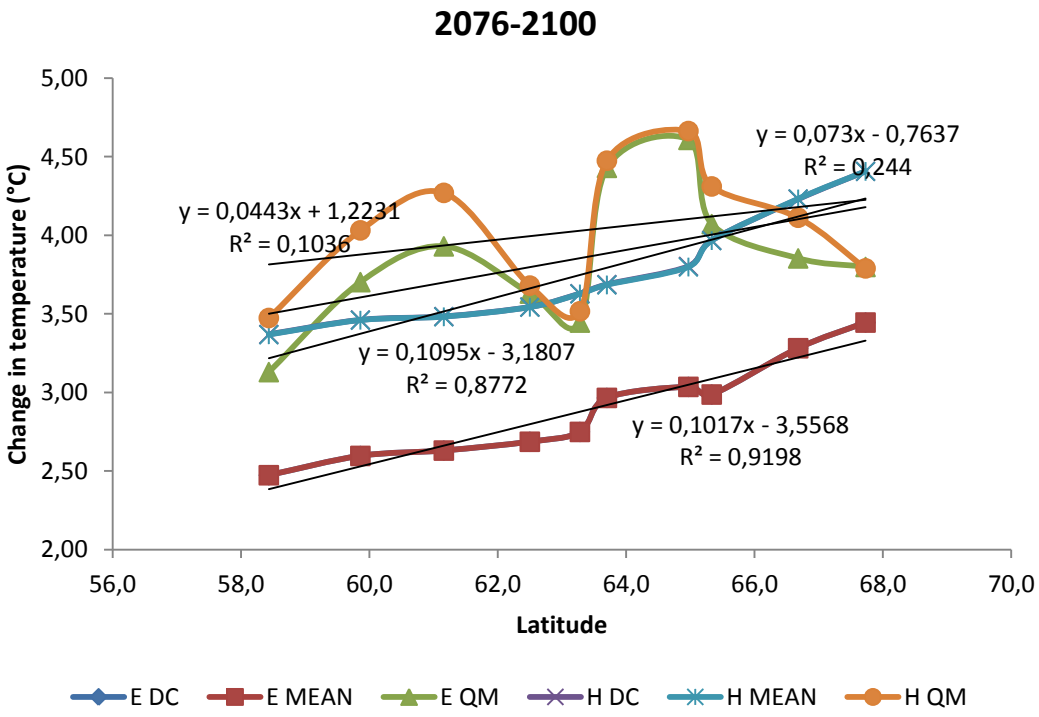

Figure 23 Change in temperature (y-axis) and measurement station latitude (x-axis) for the time period 2076-2100.

6.6 Hydrological response to use of different bias correction methods

This section serves to evaluate the hydrological response to the use of different bias correction methods by looking at the total change of inflow to the hydropower system, spring flood and lastly by showing graphs of snowpack versus inflow for all bias correction methods and time periods.

6.6.1 Total change

In this part the change in soil is calculated as the difference between the total soil for October 1st for reference and modelled data. The reason this date was chosen is that it is the beginning of the hydrological year. Soil refers to the hydropower potential of all water in the saturated and unsaturated zone

6.6.1.1 Lule

Looking at Figure 24-25 depicting the change in inflow to the hydropower system, snowpack and soil for Lule it seems the future goes towards an increase in inflow and soil, and a reduction in snowpack.

QM and DC results give the highest inflow results in both GCMs. The change occurs earlier in HADCM compared to ECHAM. In HADCM the increase for the first time period is 30-33 % and for the second 37-42 %. ECHAM results show a 16-18 % increase for the first time period and 27-35 % increase for the second.

A change in snowpack of +5 to -21 % can be seen in Figure 25 for time period one and -17 to -35 % for period two.

Soil increases 38-115 % with over 80 % of the change occurring already during the first time period. Only QM ECHAM results stand out a bit with two thirds of the change occurring during the first time period.

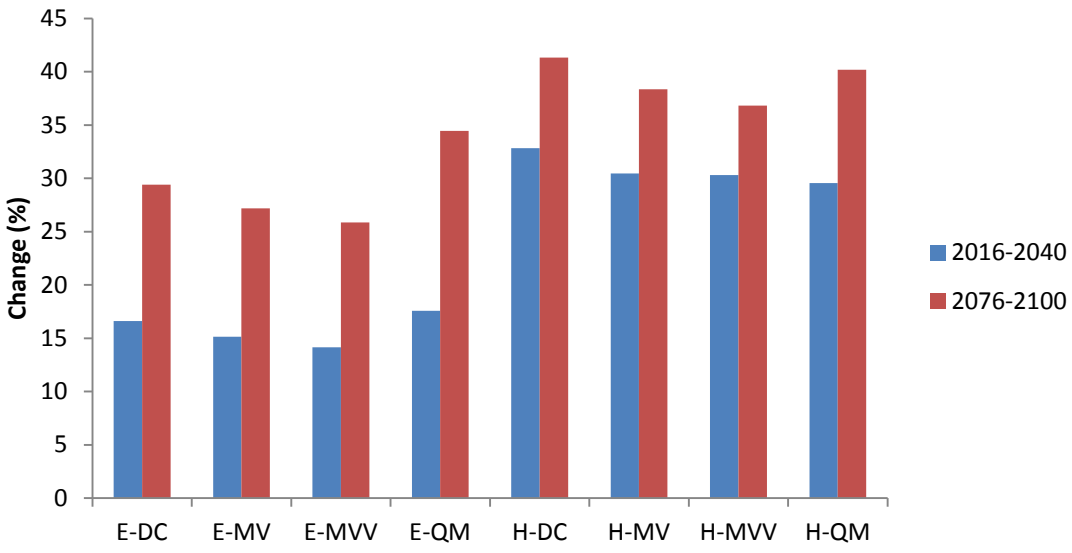

Figure 24 Change in total inflow for Lule drainage basin for time periods 2016-2040 (blue) and 2076-2100 (red), compared to reference period 1981-2005.

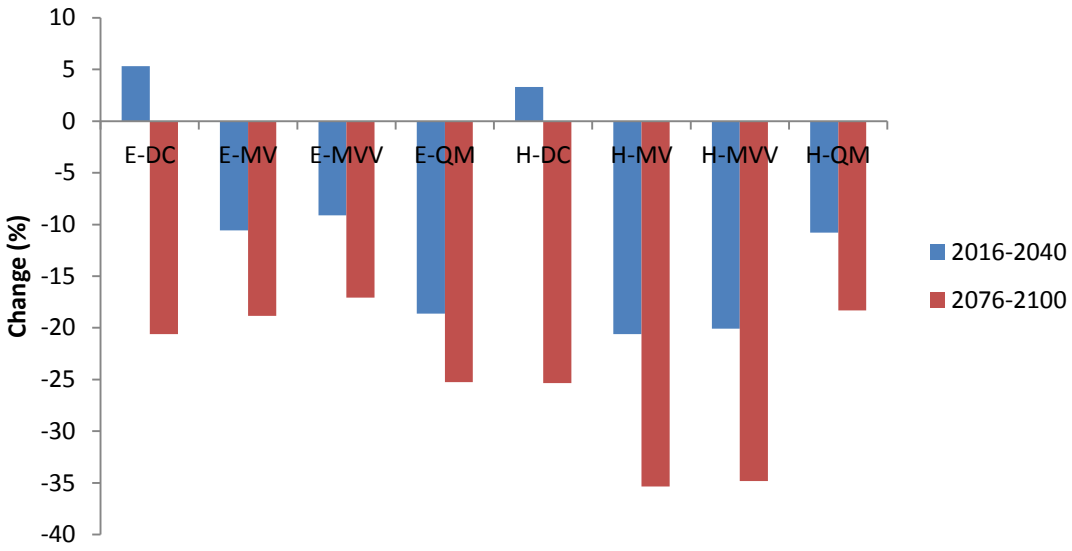

Figure 25 Change in average annual maximum snowpack for Lule drainage basin for time periods 2016-2040 (blue) and 2076-2100 (red), compared to reference period 1981-2005.

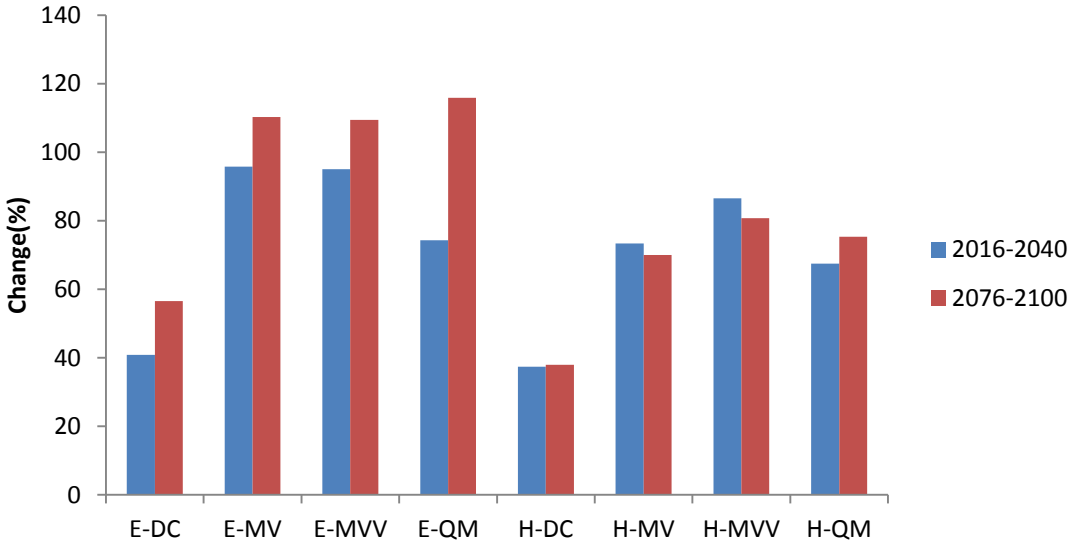

Figure 26 Change in soil at October 1st for Lule drainage basin for time periods 2016-2040 (blue) and 2076-2100 (red), compared to reference period 1981-2005.

6.6.1.2 Skellefte

In Skellefte river basin the inflow changes between -5 to +10 % during the first time period. ECHAM consistently gives the lower estimates. For the second time period the inflow increases between 5 and 21 %. All bias correction methods give very similar results, QM being the one diverting the most from the rest, Figure 27.

For Skellefte the result for change in maximum snowpack is very different for the different bias correction methods. ECHAM MV and MVV results are very similar

indicating a total decrease with 12-13 % for the first time period and 16 % the second. ECHAM DC on the other hand gives a decrease of 12 % for the first time period but a decrease of 27 % for the second. ECHAM QM gives even higher results for decrease with 28 % for the first time period and 37 for the second. This means QM results for ECHAM estimate the decrease in snowpack over 100% higher than MV and MVV for the first time period, see Figure 28.

HADCM results for snowpack are also very different for the different bias correction methods. For QM and DC the results are similar to those for ECHAM but 3-10 % higher. For MV and MVV the decrease in HADCM is twice that which ECHAM results indicated.

Soil results differ a lot depending on which bias correction method is used but are quite similar for the same methods regardless of GCM, see Figure 29.

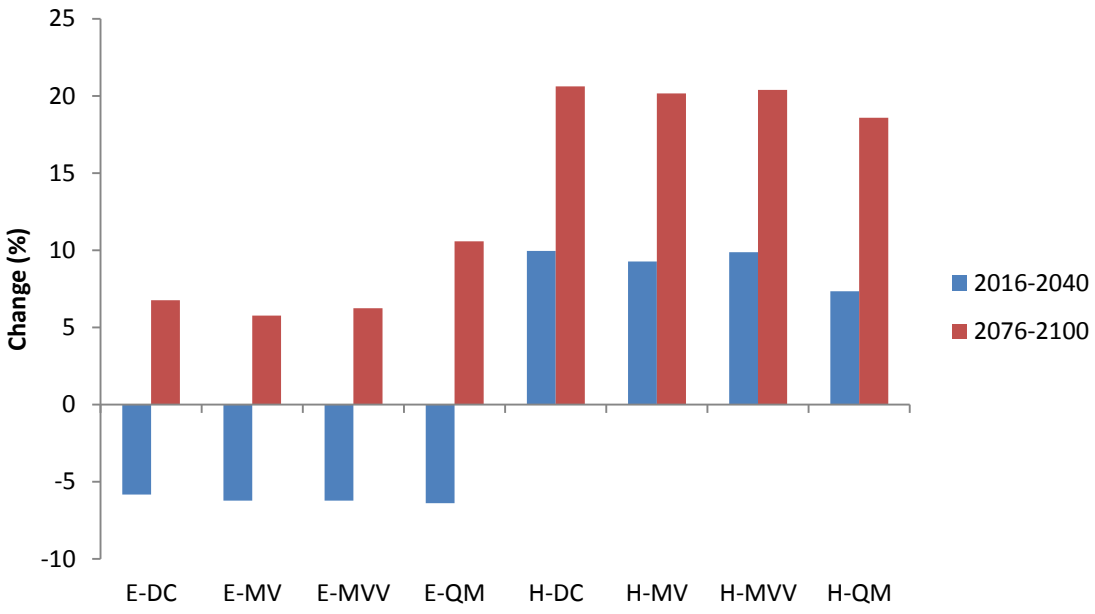

Figure 27 Change in total inflow for Skellefte drainage basin for time periods 2016-2040 (blue) and 2076-2100 (red), compared to reference period 1981-2005.

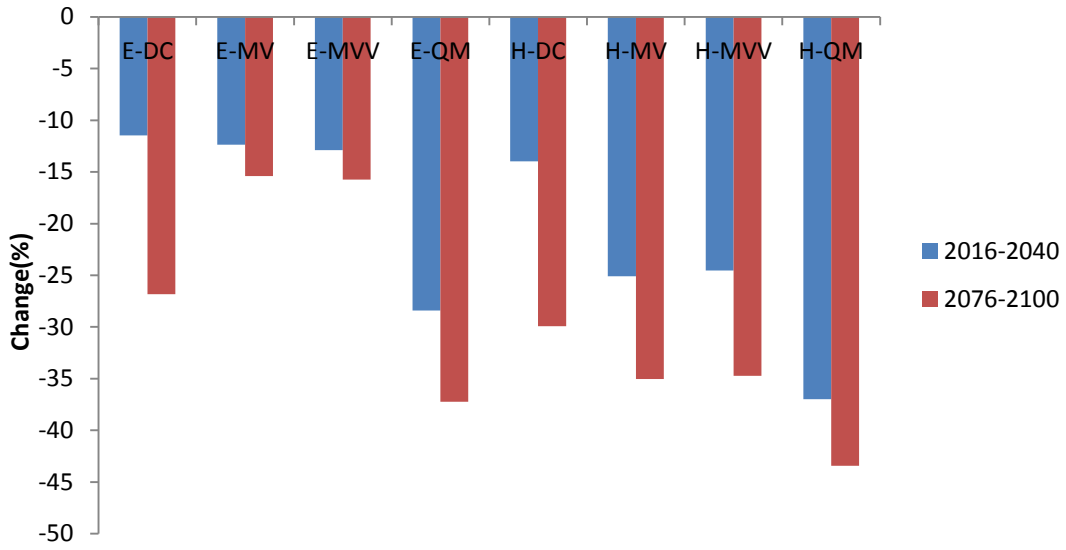

Figure 28 Change in average annual maximum snowpack for Skellefte drainage basin for time periods 2016-2040 (blue) and 2076-2100 (red), compared to reference period 1981-2005.

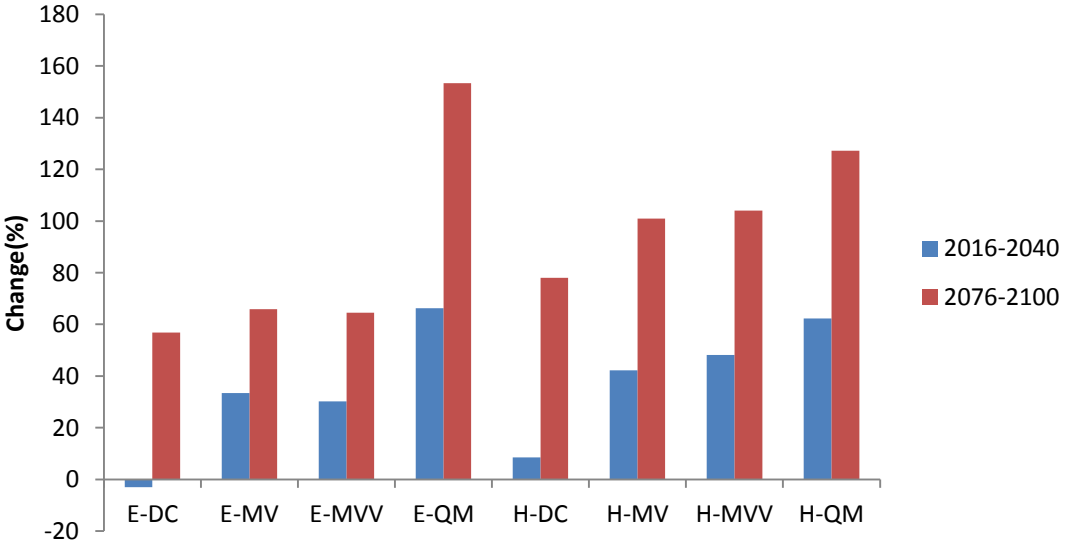

Figure 29 Change in soil at October 1st for Skellefte drainage basin for time periods 2016-2040 (blue) and 2076-2100 (red), compared to reference period 1981-2005.

6.6.1.3 Dal

For Dal the change in inflow is between -8 and +7 % for the first time period and -5 to +15 for the second time period. All ECHAM results show a decrease for both time periods and all HADCM results show an increase for both time periods, see Figure 30.

Snowpack changes with +1 - -43 % for the first time period and decreases with 14-64 % for the second time period. Interesting to note is the big difference for MV and MVV results between ECHAM and HADCM, see Figure 31.

In Figure 32 soil results are quite scattered with ECHAM giving the greatest reduction and HADCM almost no change. In ECHAM results the majority of change is visible in results for the second time period.

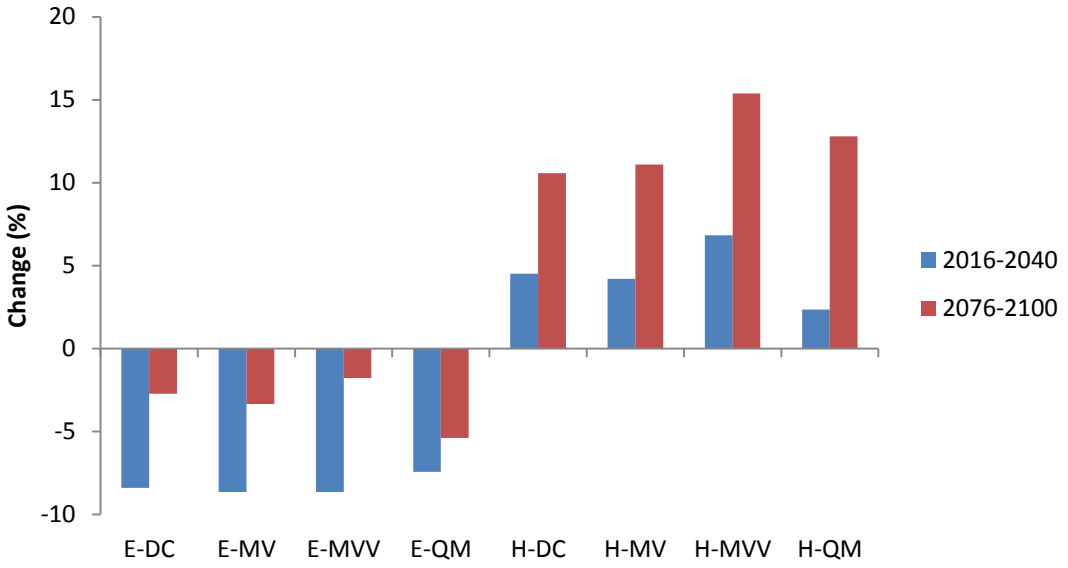

Figure 30 Change in total inflow for Dal drainage basin for time periods 2016-2040 (blue) and 2076-2100 (red), compared to reference period 1981-2005.

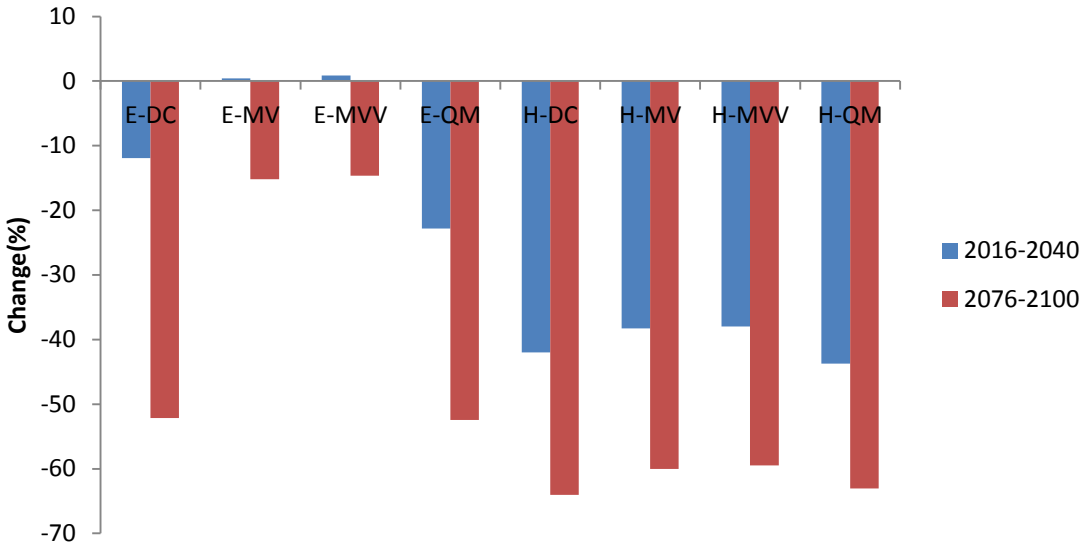

Figure 31 Change in average annual maximum snowpack for Dal drainage basin for time periods 2016-2040 (blue) and 2076-2100 (red), compared to reference period 1981-2005.

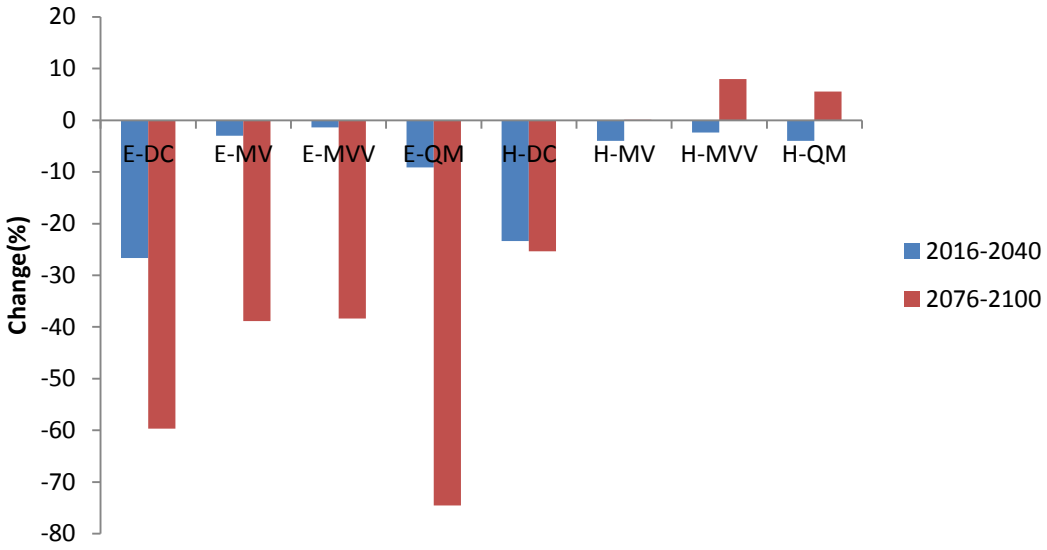

Figure 32 Change in soil at October 1st for Dal drainage basin for time periods 2016-2040 (blue) and 2076-2100 (red), compared to reference period 1981-2005.

6.6.2 Spring flood

The spring flood holds great importance to the energy price for Swedish hydropower and is therefore studied in greater detail (Österberg & Eriksson, 2004). Traditionally the spring flood is calculated between week 16-28 and the same weeks have been used in this study. An argument could be made that since the timing of the spring flood changes in the future the weeks should have been shifted a bit earlier to adjust for this, but we have chosen to study this later in the inflow versus snowpack results instead.

6.6.2.1 Lule

For Lule the total inflow during the spring weeks is about 7000 GWh and the change compared to observed data is a small overall increase of 3-17 % in the future. The change first time period is an increase of 8-18 % compared to observed and 0-17 % for the second time period compared to observed. This would indicate the spring inflow would be about the same towards the end of the century as it is during 20-16-2040, see Figure 33-34.

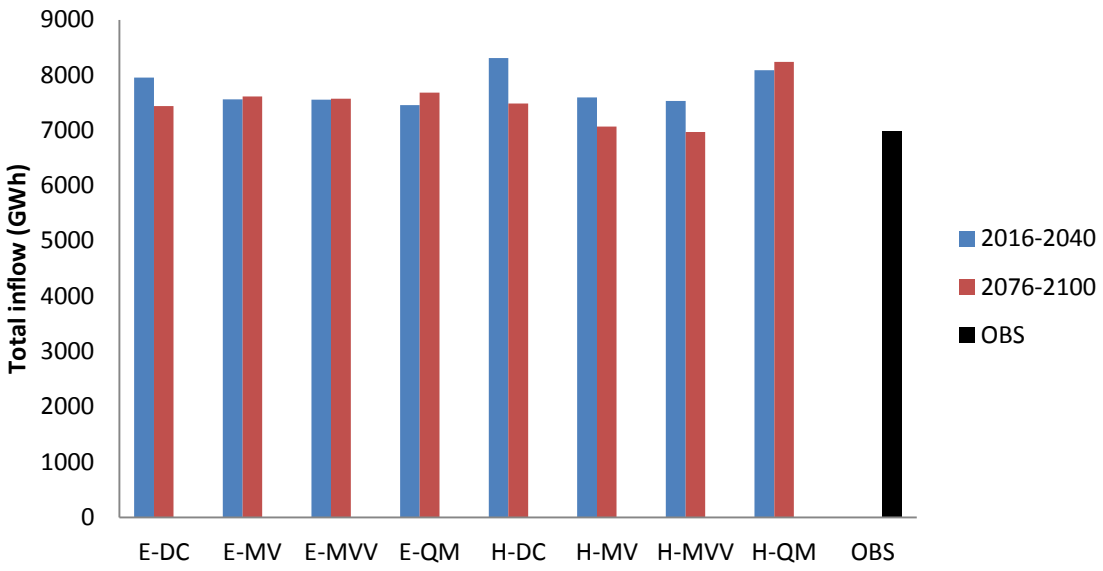

Figure 33 Lule total average spring (week 16-28) inflow in GWh for time periods 2016-2040 (blue) and 2076-2100 (red). OBS represents observed inflow for reference period 1981-2005.

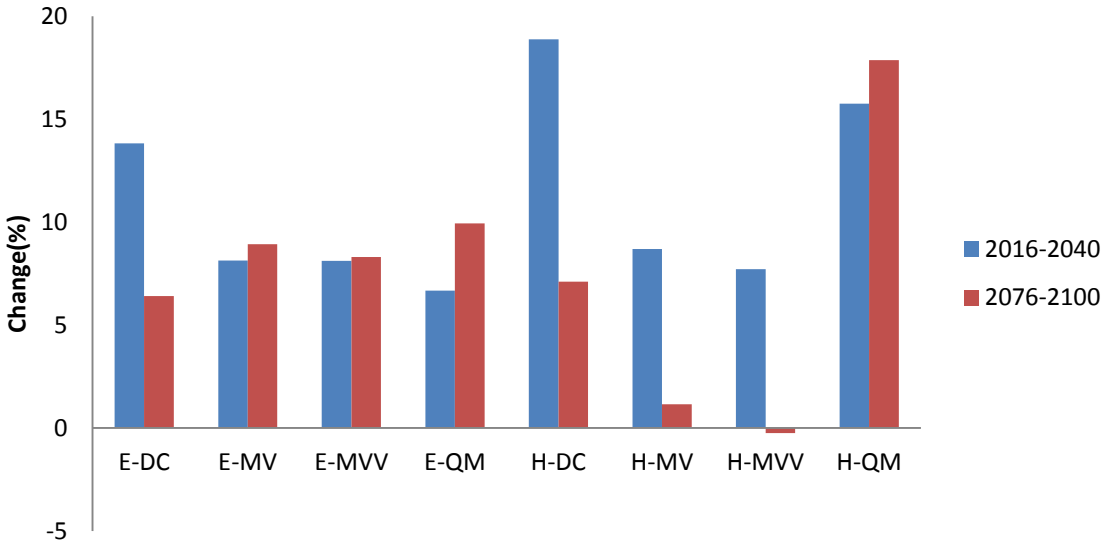

Figure 34 Lule change in total spring (week 16-28) inflow for time periods 2016-2040 (blue) and 2076-2100 (red).

6.6.2.2 Skellefte

For Skellefte the total inflow during the spring weeks is just below 2500 GWh and the change is an overall decrease of about 5-15 %. Just as was the case in Lule the decrease in inflow is the same for both time periods indicating the spring inflow will remain constant after 2040, see Figure 35-36.

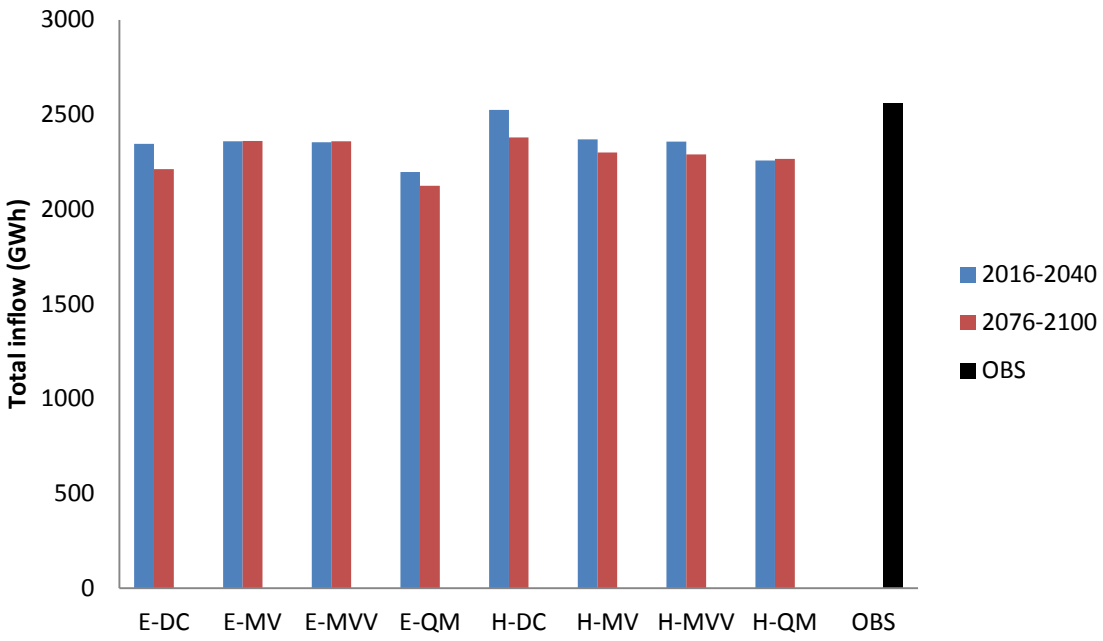

Figure 35 Skellefte total average spring (week 16-28) inflow in GWh for time periods 2016-2040 (blue) and 2076-2100 (red). OBS represents observed inflow for reference period 1981-2005.

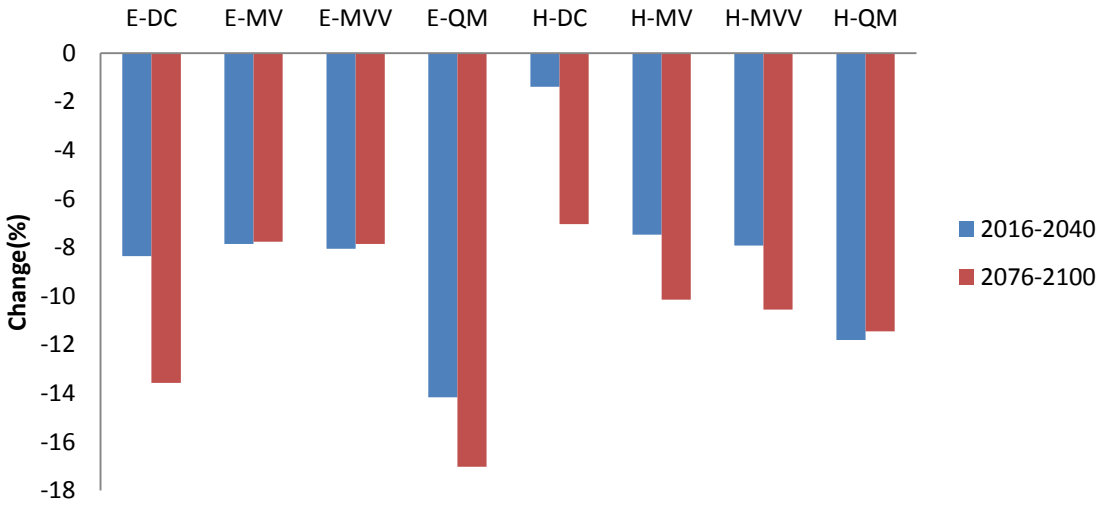

Figure 36 Skellefte change in total spring (week 16-28) inflow for time periods 2016-2040 (blue) and 2076-2100 (red).

6.6.2.3 Dal

For Dal the total inflow during the spring weeks is just below 2000 GWh and the change is an overall decrease of 5-35 %. Whether the change occurs during the first or second time period is mostly depending on which GCM was used. For ECHAM the major decrease can be seen only during the second time period. For HADCM the majority of the decrease has occurred already during the first period, see Figure 37-38.

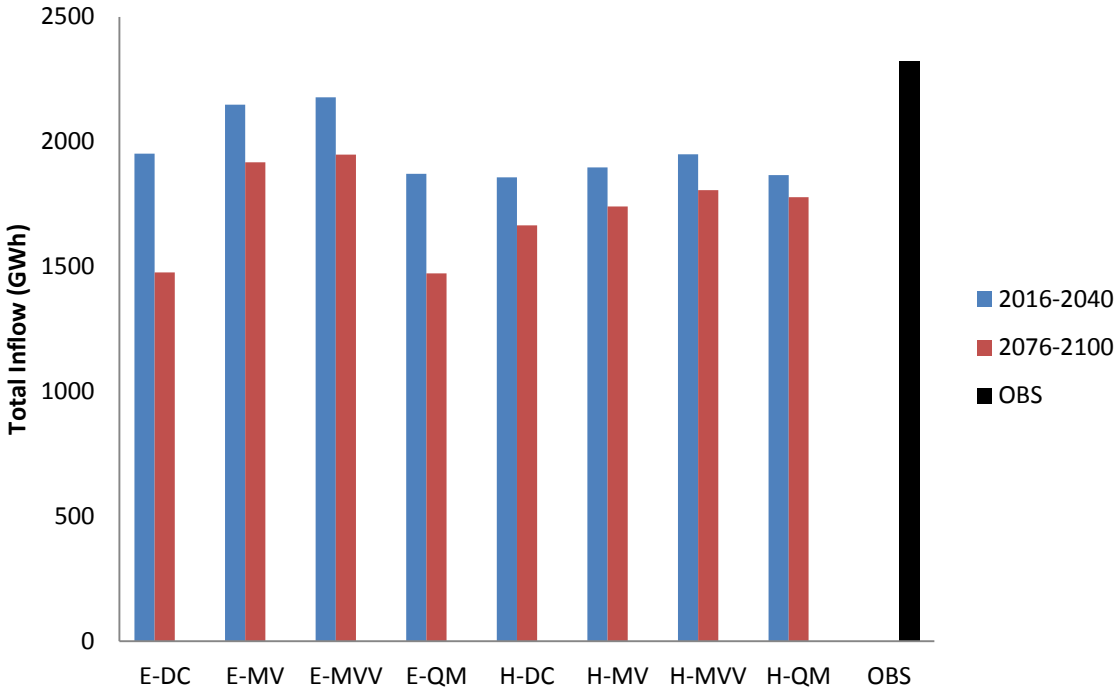

Figure 37 Dal total average spring (week 16-28) inflow in GWh for time periods 2016-2040 (blue) and 2076-2100 (red). OBS represents observed inflow for reference period 1981-2005.

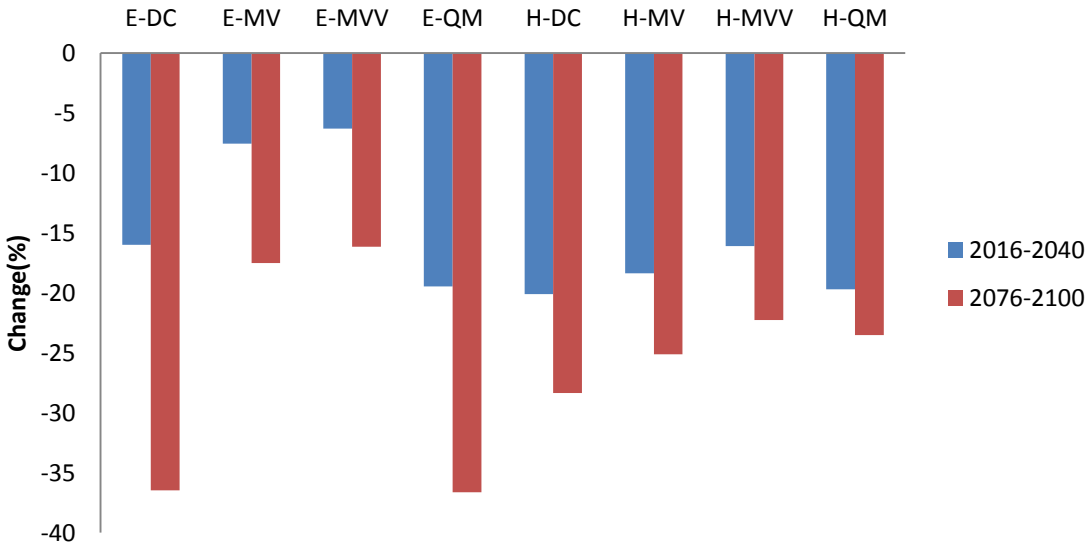

Figure 38 Dal change in total spring (week 16-28) inflow for time periods 2016-2040 (blue) and 2076-2100 (red).

6.6.3 Snowpack versus inflow

Figures with snowpack and inflow are presented in this section. One figure for each GCM, time period and river basin, are presented, so there are a total of twelve figures. Tables with timing of spring flood and volume are also presented.

6.6.3.1 Lule

As can be seen in Figure 39 during the first time period for Lule drainage basin the biggest percentage increase in flow is occurring between January and April with 0-250 %. This is however also the time period with the lowest average inflow during the year. During this period QM is the only correction method that shows an earlier spring peak, Table 13. The peak flow is higher for all bias correction methods compared to the observed and the highest is for DC with 129 GWh compared 116 in observed. QM is the bias correction that shows the highest flow during the year, except during the summer month. This is easy to understand if the results from Figure 24 and Figure 34 are steadied, they show that QM has the greatest increase in total inflow and the smallest increase during spring flood, so the increase must be bigger during other parts of the year.

Snowpack shows a slight decrease over the entire time period, especially during spring. Snowpack is decreasing for all method except DC where an increase can be seen during winter and spring. The increase in snowpack for DC can also be seen in Figure 25, an increase in maximum snowpack of five percent is found.

A hump can be seen around week six, this is a consequence of how the leap day was corrected for. A smaller number of days have been used to make the normal for the leap day, 6-7 instead of 25 days. So the normal for the leap day is higher and this effects the average week. The hump can be seen in all figures with snowpack.

In the following figure "I" stand for inflow and "S" stand for snowpack, so I-DC is the inflow for DC.

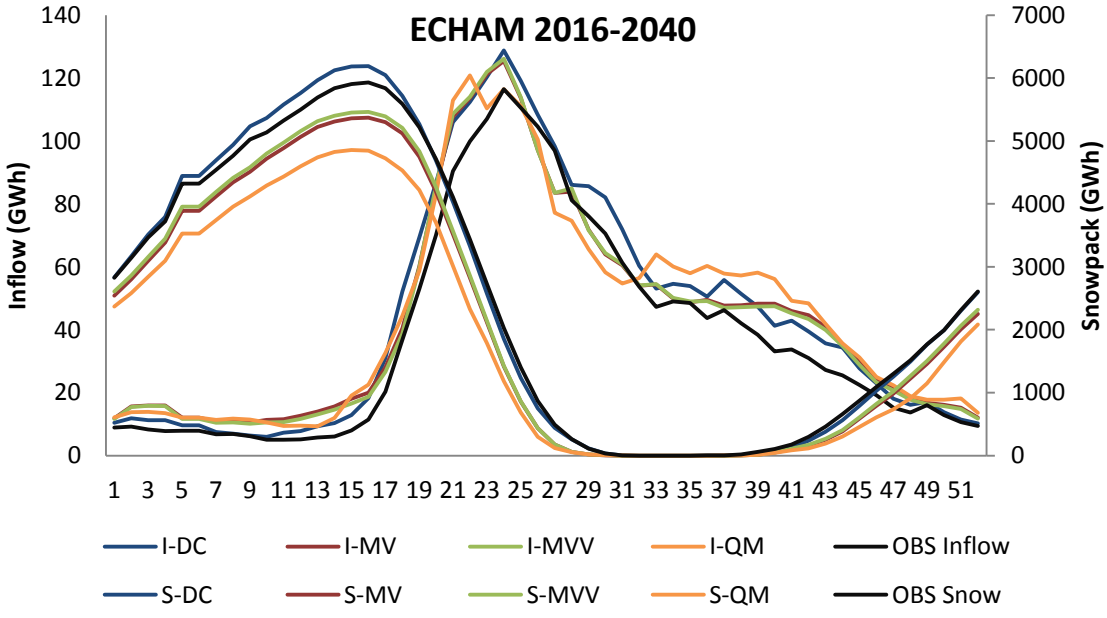

Figure 39 Lule ECHAM 2016-2040 daily average inflow (left y-axis) for each of the 52 weeks making up the average year (x-axis). Right y-axis shows the daily average snowpack for each week.

Table 13 Lule 2016-2040 ECHAM peak inflow in GWh, week that peak flow occurs, week that spring flood begins and sum of inflow during week 16-28.

ECHAM	DC	MV	MVV	QM	OBS
Peak flow (GWh)	129	125	126	121	116
Week with peak flow	24	24	24	22	24
Week start of spring flood	16	16	16	16	17
Total inflow week 16-28 (GWh)	7960	7560	7560	7460	7000

For the second time period in Lule the timing of spring peak inflow comes earlier than during the first time period, Figure 40. For the observed period the spring peak hits around week 24 and for the time period 2076-2100 it is between week 21 and 23. DC is the method with the earliest peak but also the smallest, the only one below observed peak flow. The average increase in inflow percent is also bigger compared to the first period, for the same period January-Mars the increase is now 110-350 %. The decrease during June-July is also larger than before now between 0-35 %. During autumn it seems that QM indicate higher flows than the other correction methods.

In the second time period all correction methods indicates a decrease in snowpack. The period during summer with bare ground 4-5 weeks compared to the first time period.

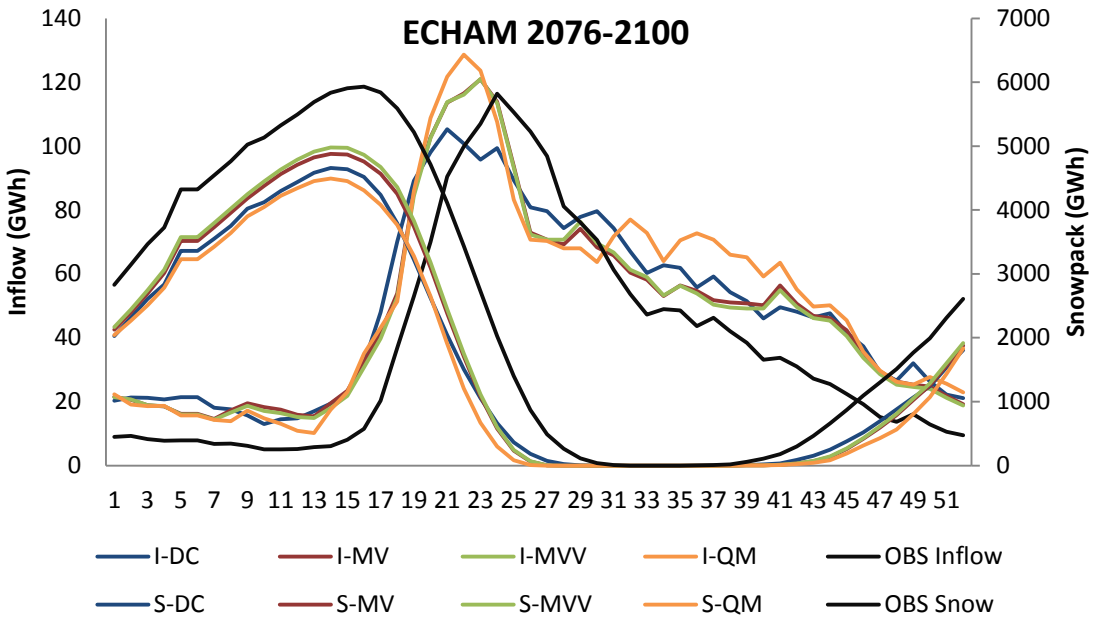

Figure 40 Lule ECHAM 2076-2100 daily average inflow (left y-axis) for each of the 52 weeks making up the average year (x-axis). Right y-axis shows the daily average snowpack for each week.

Table 14 Lule 2076-2100 ECHAM peak inflow in GWh, week that peak flow occurs, week that spring flood begins and sum of inflow during week 16-28.

ECHAM	DC	MV	MVV	QM	OBS
Peak flow (GWh)	105	121	121	129	116

Week with peak flow	21	23	23	22	24
Week start of spring flood	15	15	15	14	17
Total inflow week 16-28 (GWh)	7440	7610	7570	7680	7000

Other similar studies have often concluded a decrease in spring peak flows e.g. Andreasson et. al. (2004). To see why our results show an increase for some catchments and bias correction methods those catchments with the biggest increase of spring peak inflow compared to observed were studied in greater detail.

In Figure 41 the average daily rain for the weeks 13-25 are plotted and in Table 15 the total precipitation in the form of rain during that period is presented. QM is the correction method that has the highest spring peak inflow compared to observed and it is interesting to see that QM also indicate 500 GWh more rain than the other methods and close to 1800 GWh more than observed. This indicates the high peak in ECHAM QM results for Lule during the second time period is due to a large increase in precipitation in the form of rain compared to observed. DC, MV and MVV show similar results for rain around 1300 GWh more than observed, but MV and MVV has more accumulated snow compared to DC which could explain why those two methods peak higher.

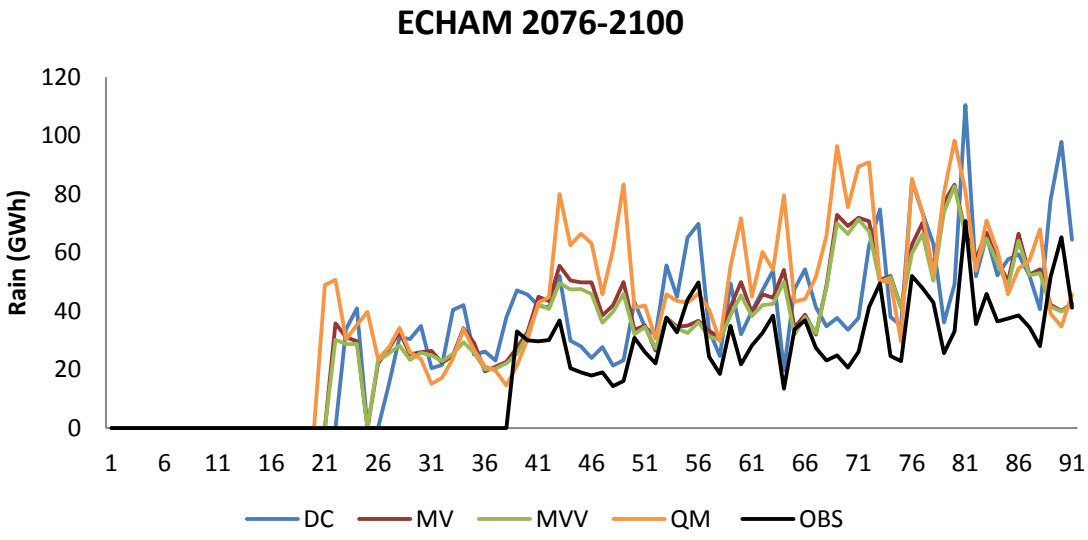

Figure 41 Lule ECHAM 2076-2100 the precipitation that comes as rain from week 13-25 for all correction methods compared to observed rain.

Table 15 Lule ECHAM 2076-2100 total precipitation in the form of rain during week 13-25 for all bias correction methods and observed.

	DC	MV	MVV	QM	OBS
Sum Rain (GWh)	2980	3020	2900	3530	1740

In the HADCM for the first time period (Figure 42) it can be seen that QM and DC are the two methods that indicate a higher spring peak value for inflow. The timing for the peak

only change for MVV, see Table 16. During winter and early spring the flow increase for all methods, the increase varies from 100-320 %. The flow is higher during summer for all methods, except MV and MVV that show a decrease compared to observed for a short period after the spring flood.

DC is the only correction method indicates a bigger snowpack during any part of the year. The increase this can also be seen in Figure 25. MV and MVV are almost identical and QM is something in between them and DC. MV and MVV are the two methods that indicate the biggest increase in time with bare ground, two-three weeks more than for observed snowpack.

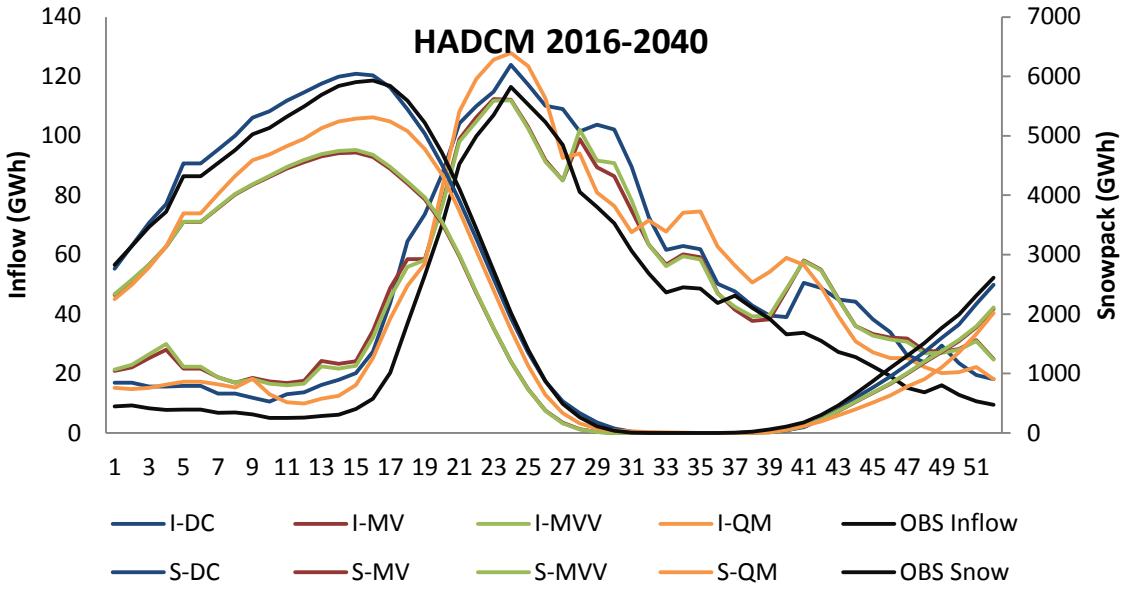

Figure 42 Lule HADCM 2016-2040 daily average inflow (left y-axis) for each of the 52 weeks making up the average year (x-axis). Right y-axis shows the daily average snowpack for each week.

Table 16 Lule 2016-2040 HADCM peak inflow in GWh, week that peak flow occurs, week that spring flood begins and sum of inflow during week 16-28.

HADCM	DC	MV	MVV	QM	OBS
Peak flow (GWh)	124	112	112	128	116
Week with peak flow	24	23	24	24	24
Week start of spring flood	15	15	15	15	17
Total inflow week 16-28 (GWh)	8310	7600	7530	8090	7000

For the second time period QM is the correction method that diverts most from the others, see Figure 43. The spring flood arrives earlier for all methods, but QM is the only one with an increase in flow 136 GWh, Table 17. During winter and spring before the peak all correction methods indicates a higher flow. The flow in winter is 100-400 % higher than during the observed period. After spring flood has occurred the flow for the correction methods all go under the observed flow, week 25-28, the decrease is

between -1 to -40 % compared to observed values. During the rest of the year all methods indicate an increase in flow, QM is the highest during summer and the lowest during autumn.

The snowpack is decreasing during the time period. The difference between the correction methods is most visible during spring, QM is higher compared to the others and after reaching its maximum the snow melt rate is higher than for the other methods. The time during summer and autumn with bare ground has increase with 5-7 weeks.

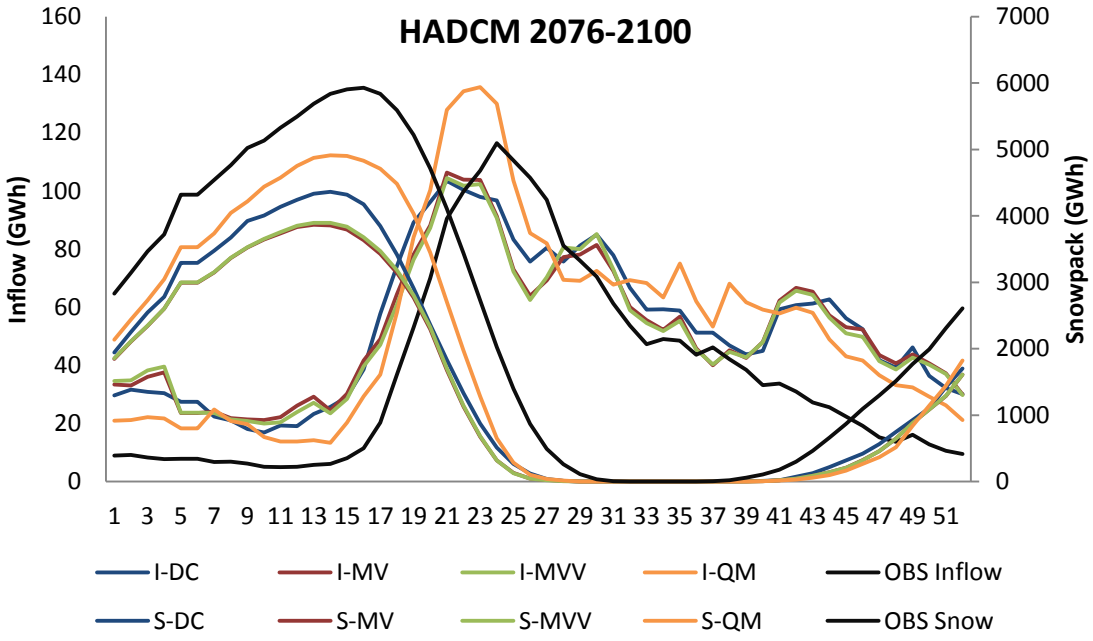

Figure 43 Lule HADCM 2076-2100 daily average inflow (left y-axis) for each of the 52 weeks making up the average year (x-axis). Right y-axis shows the daily average snowpack for each week.

Table 17 Lule 2076-2100 HADCM peak inflow in GWh, week that peak flow occurs, week that spring flood begins and sum of inflow during week 16-28.

HADCM	DC	MV	MVV	QM	OBS
Peak flow (GWh)	103	106	104	136	116
Week with peak flow	21	21	21	23	24
Week start of spring flood	14	14	14	15	17
Total inflow week 16-28 (GWh)	7490	7070	6970	8240	7000

The Lule HADCM results for the second time period also show a surprisingly high spring peak inflow in the QM results. In Figure 44 the average daily rain during week 13-25 is plotted for all bias correction methods and observed. It can be seen the QM has the highest rainfall peaks compared to the other bias correction methods.

In Table 18 showing the sum of rain during week 13-25 it can be seen that the rain for all methods varies between 3320-3560 GWh compared to observed rain of 1740 GWh. QM shows the highest increase compared to observed, over 1800 GWh. An interesting side note is how the precipitation in the form of rain is almost twice as high in the future for MV, MVV and DC compared to observed, and still all of those methods show lower spring peak inflows. This shows the importance of snowmelt and how much it governs the spring flood.

Figure 45 shows the average daily temperature during week 13-25 meaning day one in the picture is the first day week 13. QM is the correction method with the lowest temperature in the beginning, but after about 50 days it picks up and the last weeks it shows the highest temperature which could explain the rapid snowmelt seen in Figure 43.

Overall the peak of QM is explained by several factors. The larger individual rainfall events seen in Figure 44 which might lead to more overland flow and less infiltration and evaporation coupled with the fact that QM has higher snowpack than MV, MVV and DC and more rapid snowmelt.

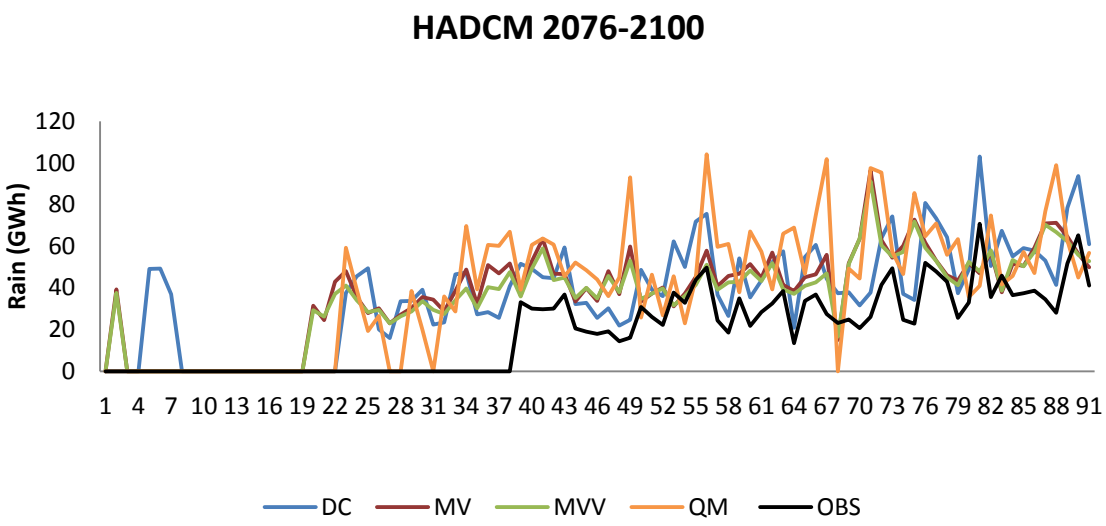

Figure 44 Lule HADCM 2076-2100 the precipitation that comes as rain from week 13- 25 for all correction methods compared to observed rain.

Table 18 Summarized rain during the period in Figure 44.

	DC	MV	MVV	QM	OBS
Sum Rain (GWh)	3340	3370	3220	3560	1740

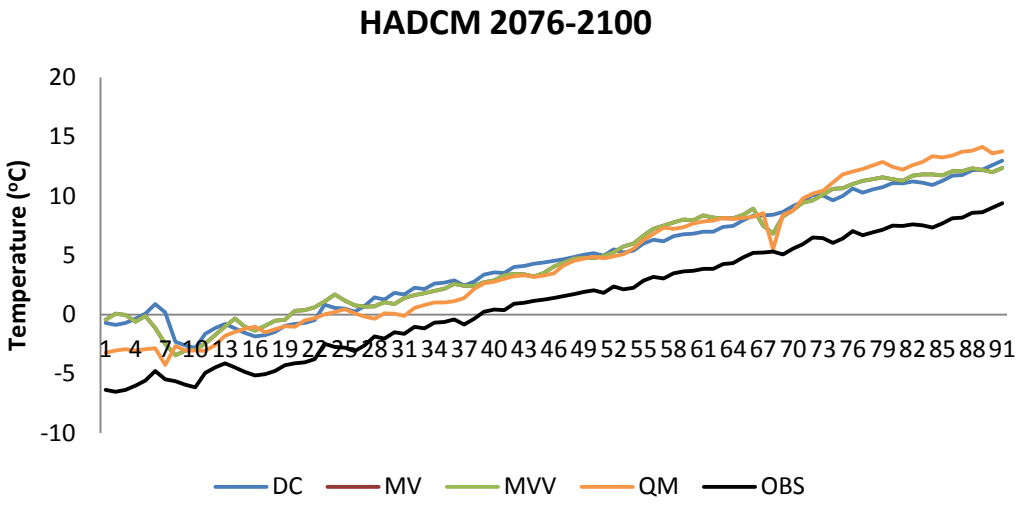

Figure 45 Lule HADCM 2076-2100 the temperature for all correction methods and observed for week 13-25.

6.6.3.2 Skellefte

Looking at snowpack results for ECHAM during the first period (Figure 46) DC, MV and MVV follow each other with a peak around 1600 GWh and QM diverts with a lower peak at 1200 GWh interesting to note is that although DC has a higher snowpack it still amounts to a lower peak flow. Although peak flow occurs during the same week as in the observed results the decline in flow after the peak is much faster for all correction methods in the future. Peak flow (Table 19) increases according to MV and MVV and decreases according to DC, QM shows no change compared to observed. The timing of the spring flood is unchanged.

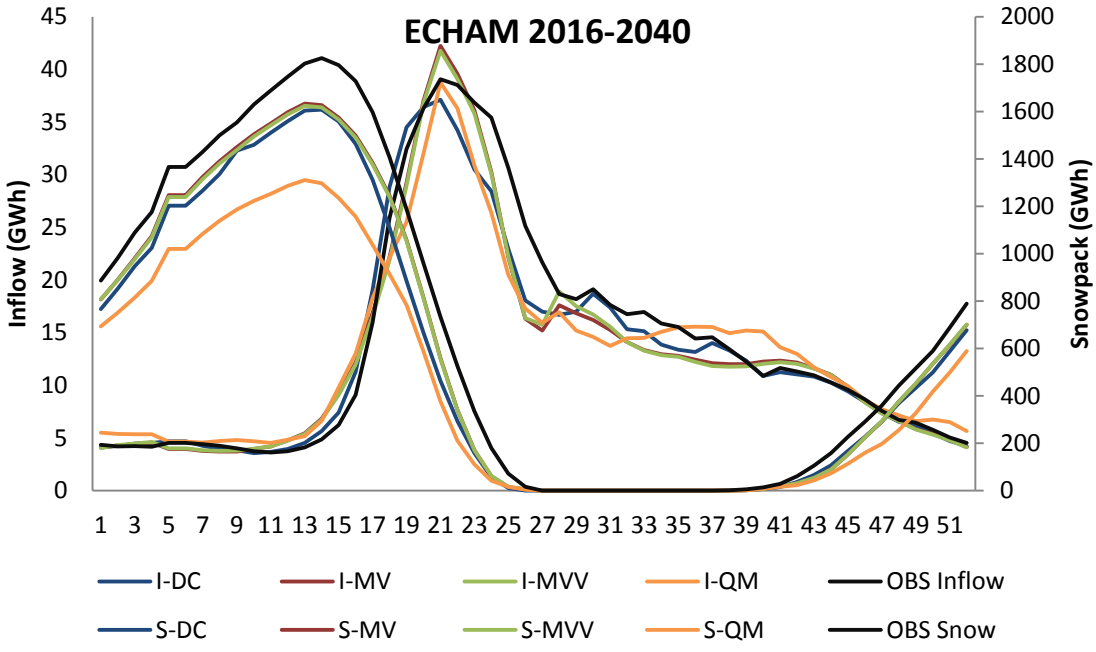

Figure 46 Skellefte ECHAM 2016-2040 daily average inflow (left y-axis) for each of the 52 weeks making up the average year (x-axis). Right y-axis shows the daily average snowpack for each week.

Table 19 Skellefte 2016-2040 ECHAM peak inflow in GWh, week that peak flow occurs, week that spring flood begins and sum of inflow during week 16-28.

ECHAM	DC	MV	MVV	QM	OBS
Peak flow (GWh)	37	42	42	39	39
Week with peak flow	21	21	21	21	21
Week start of spring flood	16	15	15	15	16
Total inflow week 16-28 (GWh)	2350	2360	2350	2200	2560

For the second time period of ECHAM snowpack results MV and MVV are relatively unchanged compared to the first time period whereas DC and QM has decreased even more (Figure 47). MV and MVV also show a higher peak flow compared to the other two methods (Table 20). As for the first time period QM shows the highest overall increase compared to observed especially during August – October. The spring peak occurs two weeks earlier according to DC and one week according to the other methods (Table 20).

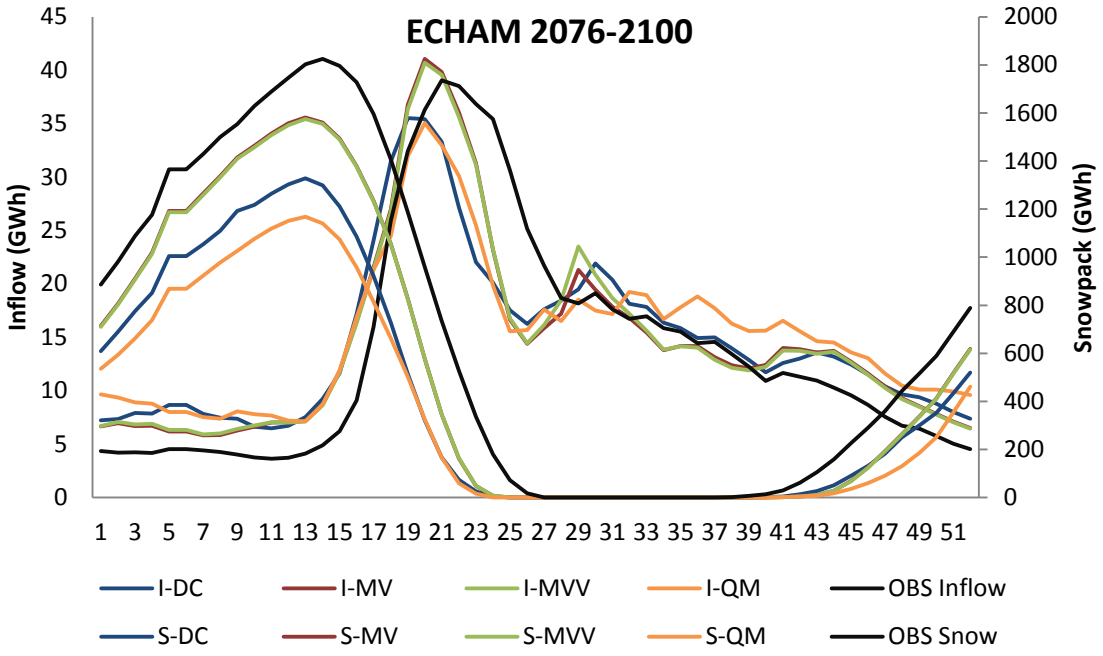

Figure 47 Skellefte ECHAM 2076-2100 daily average inflow (left y-axis) for each of the 52 weeks making up the average year (x-axis). Right y-axis shows the daily average snowpack for each week.

Table 20 Skellefte 2076-2100 ECHAM peak inflow in GWh, week that peak flow occurs, week that spring flood begins and sum of inflow during week 16-28.

ECHAM	DC	MV	MVV	QM	OBS
Peak flow (GWh)	36	41	41	35	39
Week with peak flow	19	20	20	20	21
Week start of spring flood	14	14	14	14	17
Total inflow week 16-28 (GWh)	2210	2360	2360	2120	2560

The high peak inflow in Figure 47 for MV and MVV merit further investigation. In Figure 48 the average daily rain for week 12-22 is plotted and the summarized rain is presented in Table 21. The rain is highest for QM with 820 GWh, the other have around 700 GWh, so the high peaks for MV and MVV can not only be explained by the amount of rain. Above it can be seen that MV and MVV are the two methods with the biggest snowpack and that the snowmelt is faster than for DC and QM so the high peak is mostly likely a consequence of the fast melt rate of the snowpack. It can also be seen that the peak in spring inflow in Figure 47 declines earlier than for the observed which makes sense based on the larger size and slower melt rate of the observed snowpack.

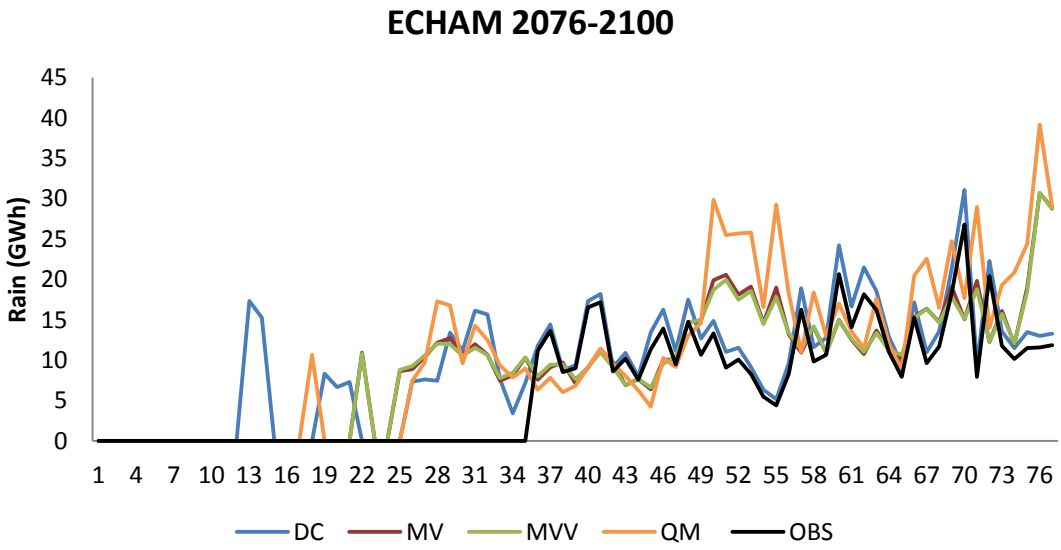

Figure 48 Skellefte ECHAM 2076-2100 the precipitation that comes as rain from week 12-22 for all correction methods compared to observed rain.

Table 21 The summarized rain during the period in Figure 48.

	DC	MV	MVV	QM	OBS
Sum Rain (GWh)	740	710	700	820	510

For the first time period of HADCM snowpack results DC show the smallest decrease, QM the biggest and MV and MVV somewhere in between. All correction methods show very similar results with regards to timing of the spring peak and size of spring peak. All show a lower spring peak compared to observed, DC with 37 GWh and the other three with 36 GWh. DC, MV and MVV show a peak week 28-32 with values 5-8 GWh higher than QM results. Table 22 shows the timing of the spring peak is unchanged for all correction methods.

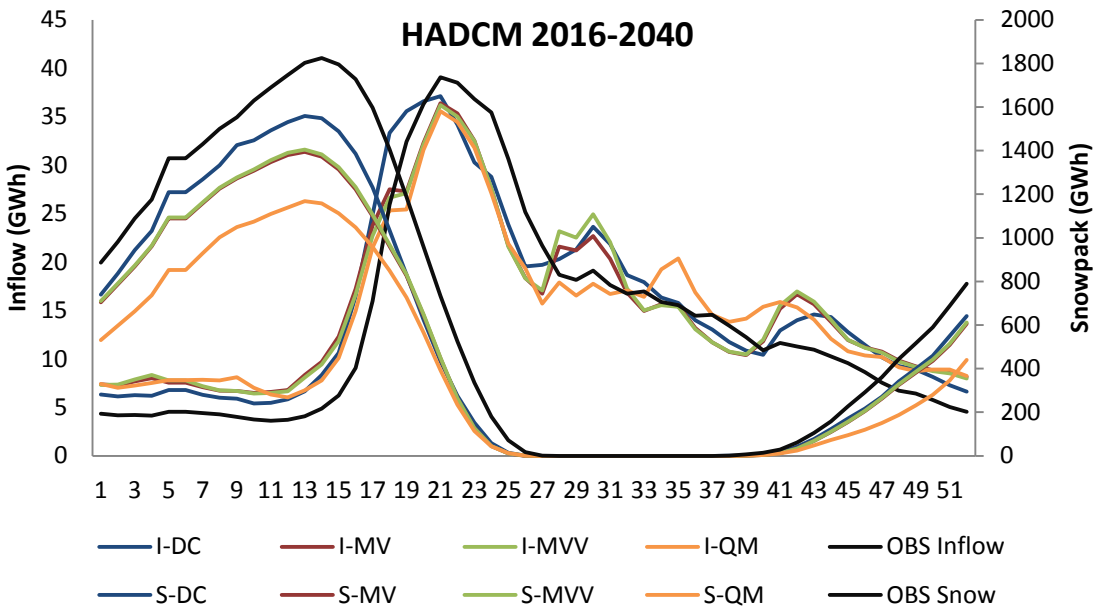

Figure 49 Skellefte HADCM 2016-2040 daily average inflow (left y-axis) for each of the 52 weeks making up the average year (x-axis). Right y-axis shows the daily average snowpack for each week.

Table 22 Skellefte 2016-2040 HADCM peak inflow in GWh, week that peak flow occurs, week that spring flood begins and sum of inflow during week 16-28.

HADCM	DC	MV	MVV	QM	OBS
Peak flow (GWh)	37	36	36	36	39
Week with peak flow	21	21	21	21	21
Week start of spring flood	15	14	14	15	17
Total inflow week 16-28 (GWh)	2520	2370	2360	2260	2560

For the second time period of HADCM inflow results DC, MV and MVV show a similar decrease in spring peak from 42 GWh in observed to 26-27 GWh. QM spring flood decreases even more down to 23 GWh. The peak around week 29 seen in Figure 49 has grown more pronounced during the second time period (Figure 50). The biggest overall increase of 80-160 % can be seen during week 43-16. The number of weeks with bare ground has increased by five weeks compared to observed data. As can be seen in Table 23 HADCM results for the second time period indicate a decrease in spring peak for all correction methods. The peak occurs two weeks earlier according to DC and is unchanged compared to observed for MV, MVV and QM.

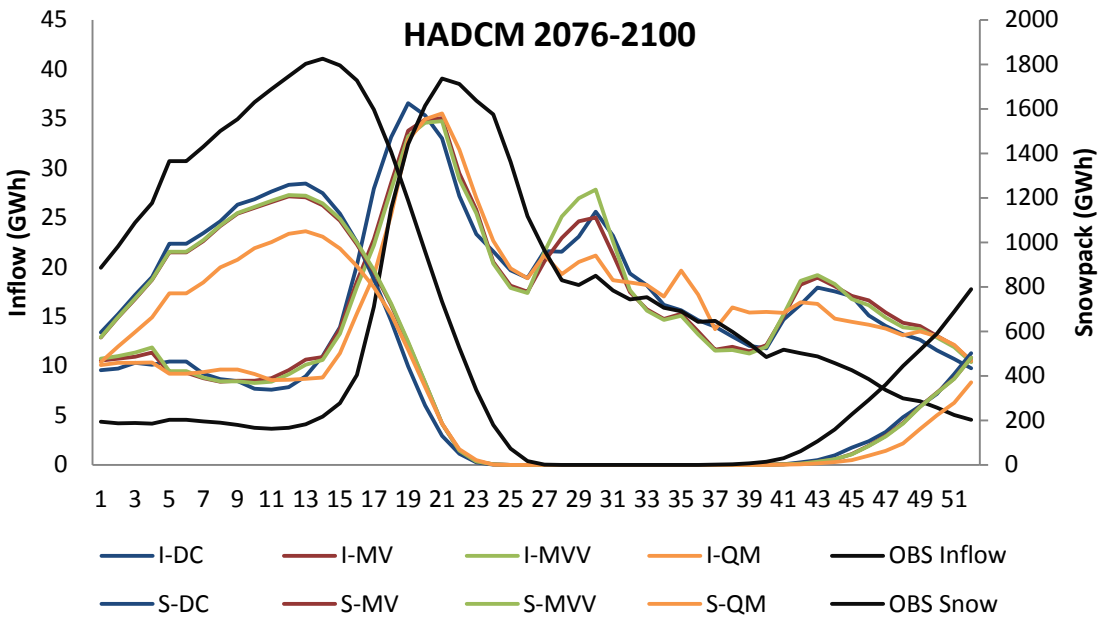

Figure 50 Skellefte HADCM 2076-2100 daily average inflow (left y-axis) for each of the 52 weeks making up the average year (x-axis). Right y-axis shows the daily average snowpack for each week.

Table 23 Skellefte 2076-2100 HADCM peak inflow in GWh, week that peak flow occurs, week that spring flood begins and sum of inflow during week 16-28.

HADCM	DC	MV	MVV	QM	OBS
Peak flow (GWh)	37	35	35	36	39
Week with peak flow	19	21	21	21	21
Week start of spring flood	14	14	14	14	17
Total inflow week 16-28 (GWh)	2380	2300	2290	2270	2560

6.6.3.3 Dal

The ECHAM snowpack results for Dal during the first time period (Figure 51) indicate an increase for MV and MVV and a decrease for DC and QM. Apart from the peak flow period all correction methods show a relatively similar distribution over the year indicating a decrease in total inflow compared to observed. Table 24 show a spring peak flow that is relatively unchanged for MV and MVV and has decreased by seven and nine GWh for DC and QM respectively. The spring peak occurs two weeks earlier according to DC, MV and MVV and three weeks earlier according to QM.

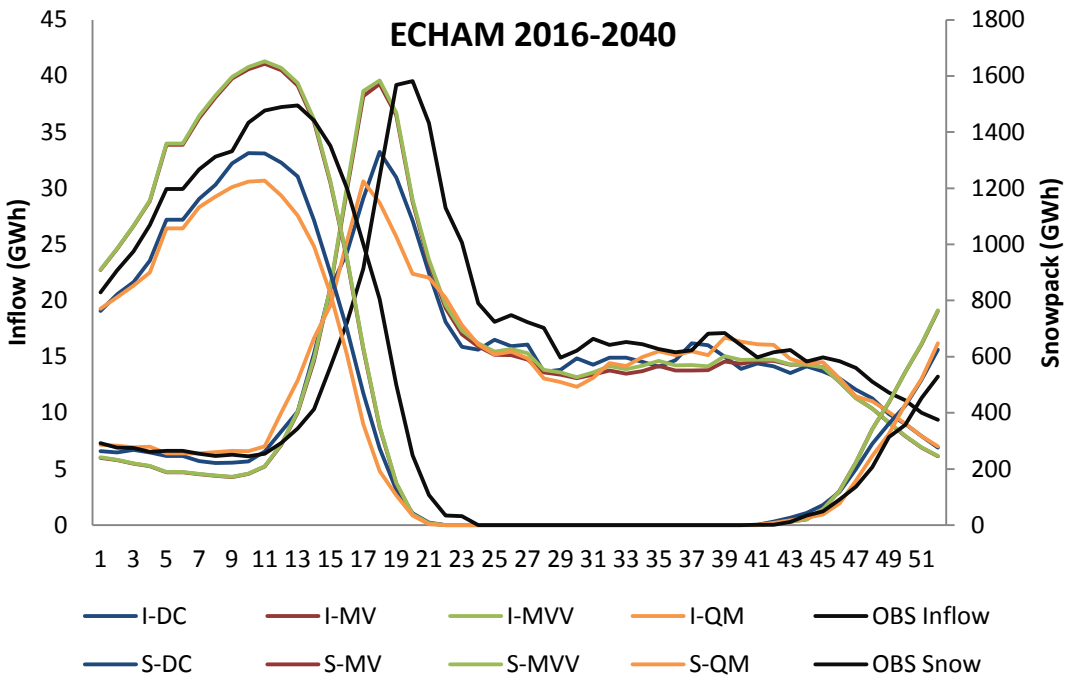

Figure 51 Dal ECHAM 2016-2040 daily average inflow (left y-axis) for each of the 52 weeks making up the average year (x-axis). Right y-axis shows the daily average snowpack for each week.

Table 24 Dal 2016-2040 ECHAM peak inflow in GWh, week that peak flow occurs, week that spring flood begins and sum of inflow during week 16-28.

ECHAM	DC	MV	MVV	QM	OBS
Peak flow (GWh)	33	39	40	31	40
Week with peak flow	18	18	18	17	20
Week start of spring flood	12	12	12	11	15
Total inflow week 16-28 (GWh)	1950	2150	2180	1870	2320

ECHAM results for the second time period (Figure 52) show very different results for the different correction methods. MV and MVV show only a slight decrease in maximum snowpack and no decrease in peak inflow. DC and QM on the other hand show a major decrease from 42 GWh in observed to 15 and 17 respectively. This is also mirrored in the peak inflow where DC and QM have decreased from 40 GWh to 22 and 24 (Table 25). All correction methods indicate an earlier peak in spring inflow, for DC its week 15 instead of week 20 in observed and for MV, MVV and QM week 17. During week 24-51 the results are relatively similar for all correction methods showing a general decrease in inflow compared to observed.

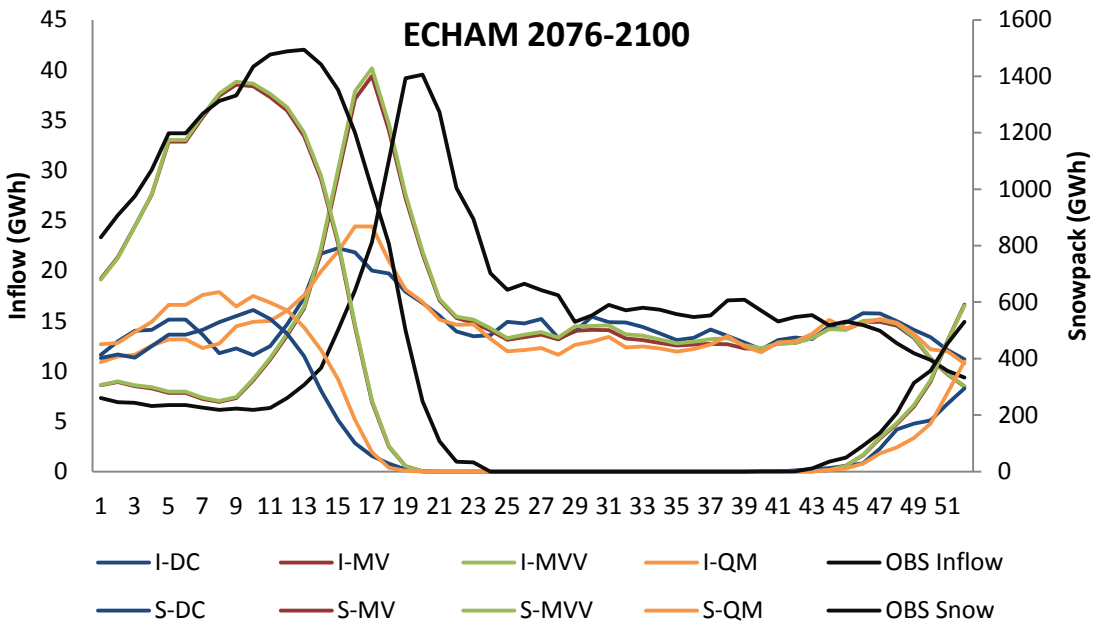

Figure 52 Dal ECHAM 2076-2100 daily average inflow (left y-axis) for each of the 52 weeks making up the average year (x-axis). Right y-axis shows the daily average snowpack for each week.

Table 25 Dal 2076-2100 ECHAM peak inflow in GWh, week that peak flow occurs, week that spring flood begins and sum of inflow during week 16-28.

ECHAM	DC	MV	MVV	QM	OBS
Peak flow (GWh)	22	39	40	24	40
Week with peak flow	15	17	17	17	20
Week start of spring flood	10	9	9	8	15
Total inflow week 16-28 (GWh)	1480	1920	1950	1480	2320

The peak of MV and MVV in Figure 52 for both snowpack and spring inflow is very high compared to DC and QM results and are therefore studied in greater detail. In Figure 53 the average daily rain during week 10-22 is plotted and in Figure 54 the temperature for the same weeks are also plotted. In Table 26 the summarized rain can be seen and the different methods indicates similar precipitation from 2120-2250 GWh compared to observed 1590 GWh.

The peak for MV and MVV cannot be explained by the increase in rainfall, however looking at the temperatures in Figure 54 there is nothing to indicate any faster snowmelt in MV and MVV compared to the other methods.

Another explanation to the higher snowpack could be that more precipitation fall during week 1-9 when snowpack accumulates and this is studied in Figure 55. Results however show no higher snowfall in MV and MVV compared to the other methods and the high peak of MV and MVV in snowpack is hard to explain.

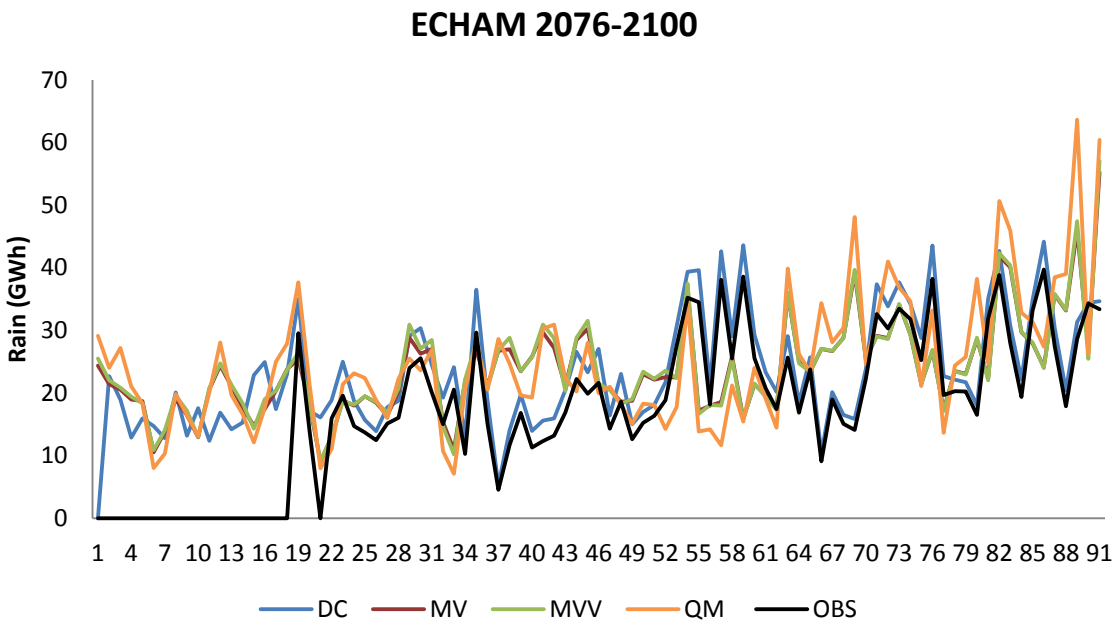

Figure 53 Dal ECHAM 2076-2100 the precipitation that comes as rain from week 10-22 for all correction methods compared to observed rain.

Table 26 Dal ECHAM 2076-2100 the summarized rain during week 10-22.

	DC	MV	MVV	QM	OBS
Sum Rain (GWh)	2120	2170	2190	2250	1590

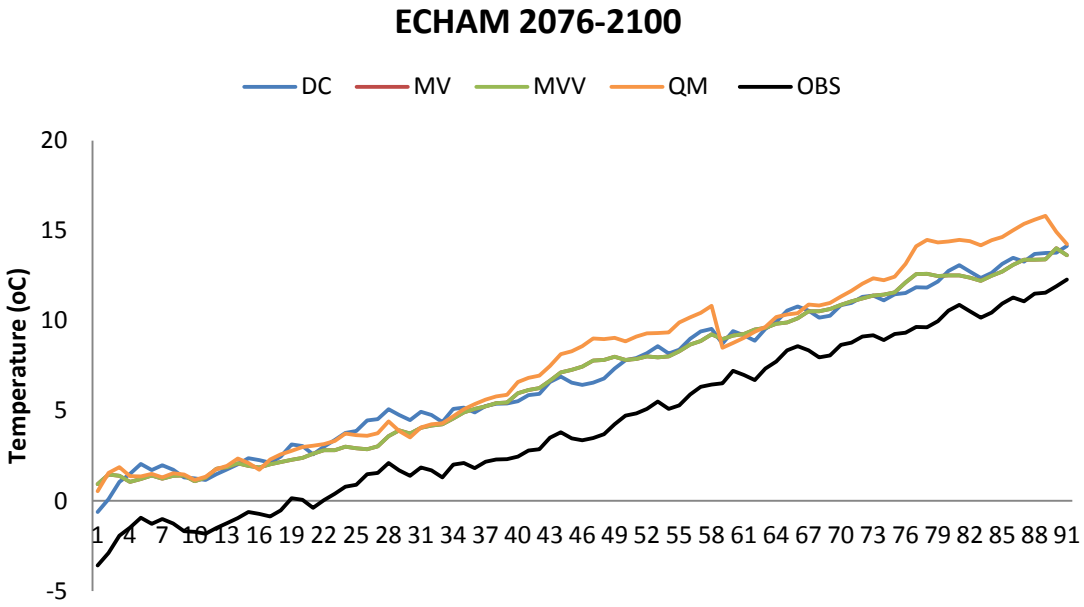

Figure 54 Dal ECHAM 2076-2100 the temperature for all correction methods and observed for week 10-22.

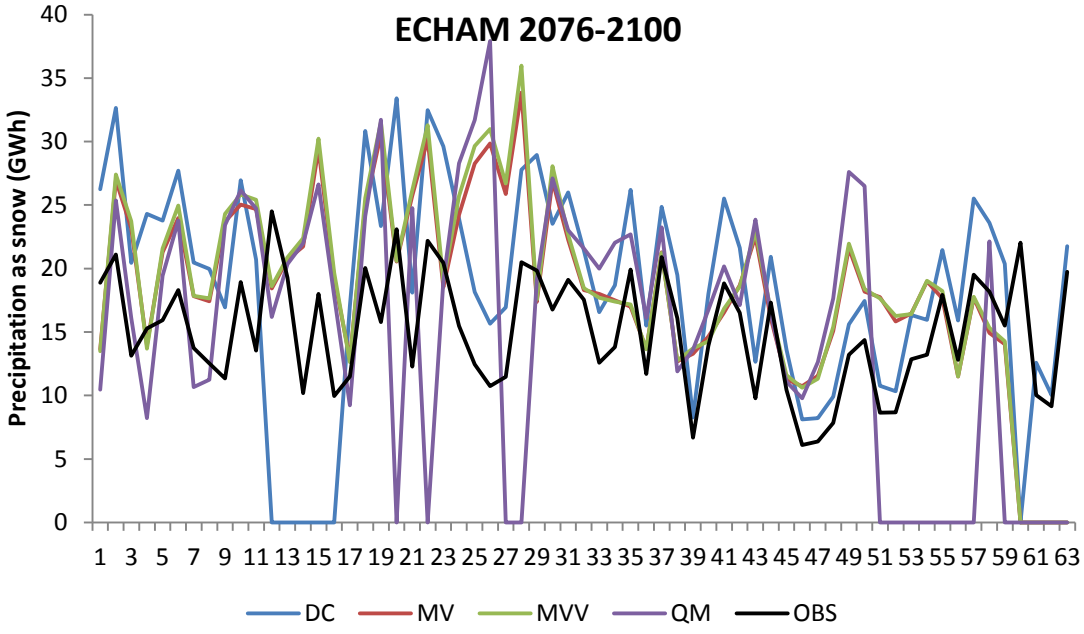

Figure 55 Precipitation in the form of snow during week 1-9. The y-axis show GWh and the x-axis days, day 1 corresponds to the first day of week one of the year plotted in Figure 52.

For Dal HADCM results it can be seen that the increase for the first time period is mostly during winter (Figure 56). The spring peak inflow arrives earlier for all correction methods and the decrease in peak flow varies from 15-23 % (Table 27). The flow during parts of summer is 50 % under the observed flows and during the rest of the year the

flow is approximately the same as the observed. The snowpack is lower than the observed for all correction methods during the whole year. The maximum for the observed is around 1500 GWh and for the correction methods 700-900 GWh. The smallest decrease in snowpack is for MV and MVV. With The time with bare ground increases with 4-6 weeks.

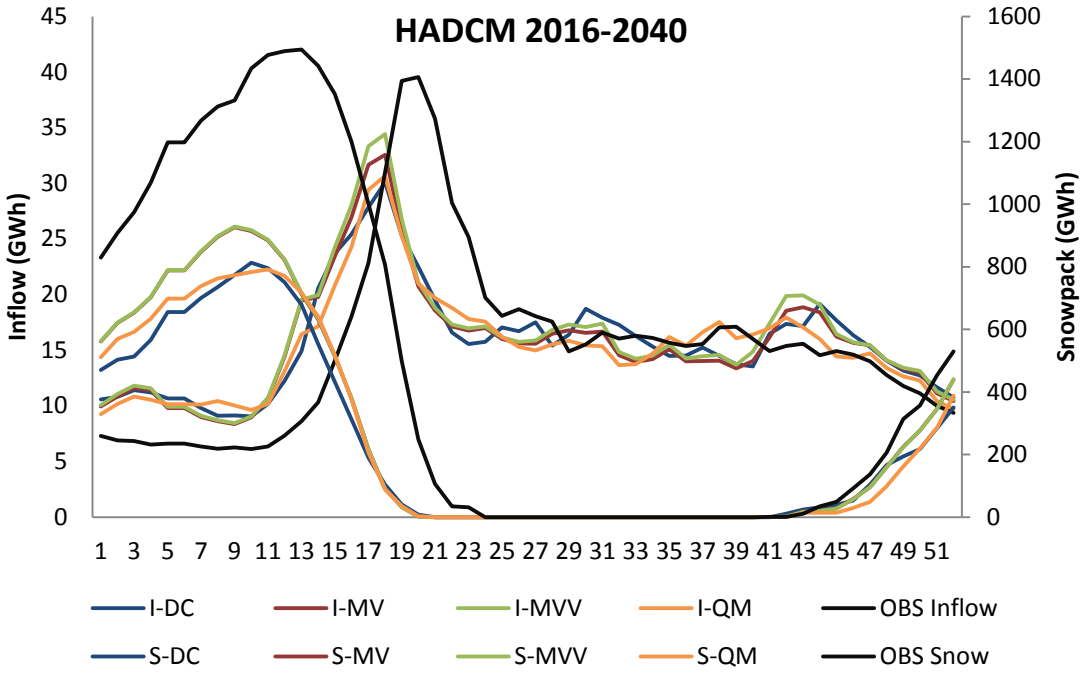

Figure 56 Dal HADCM 2016-2040 daily average inflow (left y-axis) for each of the 52 weeks making up the average year (x-axis). Right y-axis shows the daily average snowpack for each week.

Table 27 Dal 2016-2040 HADCM peak inflow in GWh, week that peak flow occurs, week that spring flood begins and sum of inflow during week 16-28.

HADCM	DC	MV	MVV	QM	OBS
Peak flow (GWh)	30	33	34	31	40
Week with peak flow	18	18	18	18	20
Week start of spring flood	11	11	11	11	15
Total inflow week 16-28 (GWh)	1860	1900	1950	1870	2320

For the second time period in Dal drainage basin flow regime over the year has changed drastically (Figure 57). Instead of an apparent spring flood as for the observed, the correction methods indicate an inflow which is relatively evenly distributed over the year varying from 14-22 GWh. The period with bare ground increase with around ten weeks compared to observed snowpack. This can also be seen in Table 28.

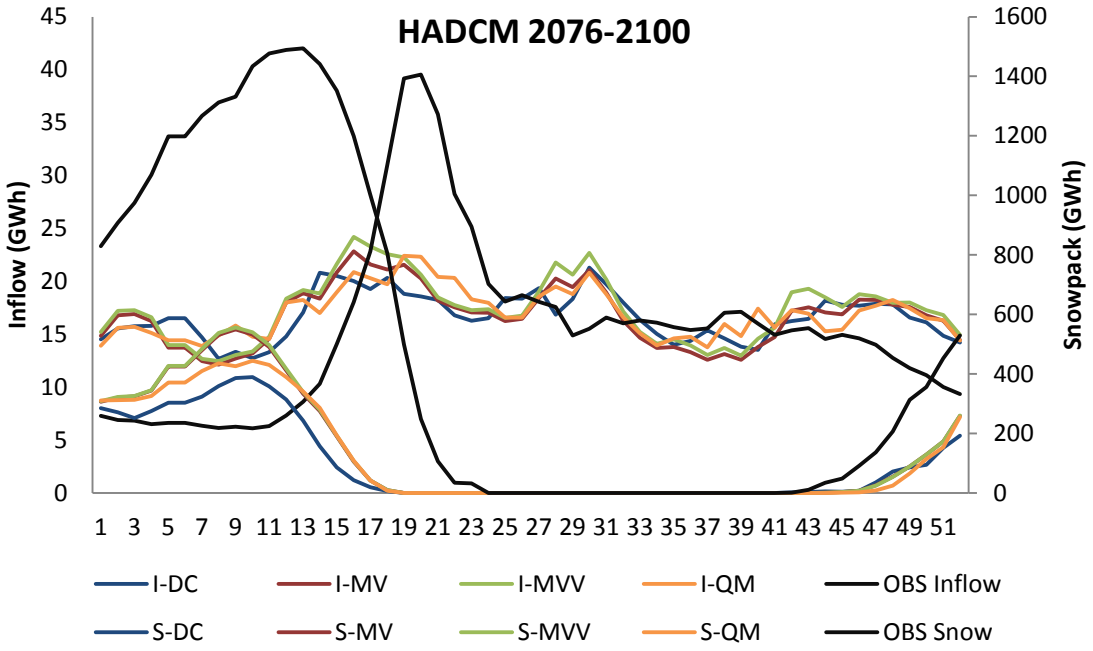

Figure 57 Dal HADCM 2076-2100 daily average inflow (left y-axis) for each of the 52 weeks making up the average year (x-axis). Right y-axis shows the daily average snowpack for each week.

Table 28 Dal 2076-2100 HADCM peak inflow in GWh, week that peak flow occurs, week that spring flood begins and sum of inflow during week 16-28.

HADCM	DC	MV	MVV	QM	OBS
Peak flow (GWh)	21	23	24	22	40
Week with peak flow	14	16	16	19	20
Week start of spring flood	10	10	10	10	15
Total inflow week 16-28 (GWh)	1670	1740	1810	1780	2320

7 Discussion and summary of results

A general note should be made with regards to all results regarding when the majority of change actually occurs. Since the first time period is 2016-2040 and the second is 2076-2100 there is a gap of 36 years between the two. This means that even if the results show an increase of 100 % for the first time period and 200 % for the second time period, the rate of change is more than twice as big for the first time period compared to the second assuming the change from 2040 and onwards was linear until the end of the century.

7.1 Precipitation

QM and DC are the two methods that indicate the highest extreme precipitation in eleven results out of twelve. DC has the weakness that it corrects all precipitation with the same factor Graham et al. (2007), whereas QM is more advanced calculating different correction factors for each percentile and fitting them into two different

polynomials one for extreme events and one for normal precipitation. Since QM got even higher results than DC it indicates the daily correction factors and the extra polynomial fitted to the top five percent in QM makes a difference.

The increase in precipitation depends mainly on which GCM that is used and which time period it is. For the first time period ECHAM indicates an interval from -1.2 to +5.1, for the second time period the interval changed to an increase with 4-22 %. The difference between the correction methods is small, but it is QM that in over 70 % of the stations indicates the highest increase compared to observed precipitation. The increase in precipitation compared to observed precipitation is higher for HADCM than for ECHAM in both periods. In the first time period for HADCM the correction methods indicates an increase interval from 9-24 %. For the second time period the increase in precipitation has changed to 16-34 %.

The difference in precipitation between the two GCMs could be either due to the climate models or the different grid size of the RCM used for downscaling. On one hand Van Roosmalen (2009) found when studying grid size impact comparing 40 km^2 and 10 km^2 gridded data that the difference in precipitation output were negligible. On the other hand Kleinn et. al (2005) concluded that gridded data with resolution 14 km presented finer and more realistic precipitation than gridded data with resolution 56 km. However no significant difference could be seen in the simulated stream flow. The difference in precipitation is therefore most likely a consequence of different representation of the study area in the two GCMs.

The mean precipitation is similar for all correction methods which indicate that when investigating total average changes the choice of bias correction is not that important. The difference between the correction methods is less than five percent for all stations. Van Roosmalen et.al (2011) compared DC and DBS and came to the same conclusion, that choices of correction method has little effect on mean changes.

QM results give the biggest interval of change when investigating monthly mean. The interval is from -30 to +79 % compared to DC, MV and MVV that show intervals from -7 to +55 %. It would seem that QMs correction of all precipitation events individually makes a difference, in our opinion giving a more realistic representation of future precipitation. The large interval of possible future precipitation evens captured by QM compared to the other methods could be especially useful for e.g. flood mitigation and dam dimensioning applications.

7.2 Temperature

The temperature will change with 0.3-2 °C for the first time period and 2.5-4.5 °C for the second. The amount of change seems mostly depending on which GCM was used except for QM for the second time period where both GCMs showed similarly high results for temperature change. DC and MV indicated a greater change in temperature the further north the measurement station was located. The temperature results are similar to those of Andreasson et. al., (2004) which indicated an increase of 2.5-4.6 degrees in Sweden towards the end of the century.

7.3 Total inflow, snowpack and soil

Looking at the total average annual inflow, the change is greater the further north the catchment is located. This conclusion was also made by Andreasson et. al. (2004) in their study of Climate change impact simulations for Sweden. An example of this is the second time period where Lule shows an increase of 26-41 %, Skellefte 5-21 % and Dal -5-+15 %. The increase in inflow for Lule was also studied by Graham et. al., (2007) looking at the climate change effects on hydropower for Lule river basin. Using the HADCM3 and ECHAM4 GCMs and several RCMS Grahams results indicated an increase from 18-59 % with an average of 34 %. The fact that Graham results indicate a larger interval is most likely because he included more emission scenarios and RCMs in the study.

For snowpack the pattern is an overall reduction. Lule and Skellefte show similar results, Lule with a decrease of 20-45 % and Skellefte 17-35 %. Dal had a greater decrease from 15-63 %.

Looking at soil results Lule shows an increase of 38-117 %, Skellefte 58-155 % and Dal a change of +8 to -72 %. For Lule the majority of the change has occurred already for the first time period whereas for Skellefte and Dal it is less than half.

There doesn't seem to be any clear connection regarding which time period where the majority of the change of inflow, snowpack and soil occurs for the different drainage basins.

7.4 Spring total inflow

Looking the total inflow during spring and the total change in spring inflow several pattern can be observed. The first is that the overall change is a greater decrease the further south the river basin is located.

For Lule it is an increase of 0-15 %, for Skellefte a decrease of 8-17 % and for Dal a decrease of -16 to -36 %. For Lule and Skellefte the majority of change occurs already for the first time period, indicating spring inflow would remain mostly unchanged after 2040.

These results for the total change during spring coupled with the previously discussed results of the total overall change also say something of when this change occurs. If the total change is an increase for Lule for example of 20-45 % and the increase during spring, which is when flow is at its peak is only 0-15 %, the change during the rest of the year has to be quite substantial.

7.5 Weekly average inflow versus snowpack coupled with monthly change in total inflow

For Lule during the first time period only two out of eight results indicate any change in the timing of spring peak and the change is 1-2 weeks earlier, for the second period all methods indicate a shift 1-3 weeks earlier. This is a bit less than the results obtained by Graham et. al., (2007) where they predicted that spring flood would arrive about one month earlier towards the end of the century.

For Skellefte there is no change during the first time period and a shift 1-2 weeks earlier according to the ECHAM results for the second time period. In the HADCM results for the second time period only DC out of the four methods indicate any change, a shift two weeks earlier.

Dal results for the first time period indicate a spring peak inflow that hits 2-3 weeks earlier compared to the observed. For the second time period the results are more scattered indicating a 1-6 week earlier spring peak.

Looking at the difference between the bias correction methods MV and MVV gave the highest peak inflow values for four out of six of the ECHAM spring results. In all cases they also showed the highest snowpack. QM indicated the highest average spring peak inflow in HADCM Lule results, in one of those cases DC showed higher snowpack.

A change can also be seen in the timing of the peak snowpack, for the first time period the size of the snowpack has gone down but the timing of the peak seems mostly unchanged. For the second time period however there is a clear shift in the timing of the maximum snowpack where it occurs one to four weeks earlier.

When it comes to the distribution of change in mean inflow over the year the general trend is the same for all river basins. The biggest increase can be seen from January-Mars with a short period of decrease sometime during May-July. The decrease seems to arrive later in the year the further north the river basin is located with June-July for Lule, June for Skellefte and May for Dal.

This is most likely related to the previously discussed reduction in snowpack and the timing of the peak flow shortly after the snowpack starts to melt. If the inflow during May-July is governed mainly by contribution from melting snow it is not strange that the reduction in snowpack during winter due to higher average temperature would have a bigger impact on the inflow than a general increase in precipitation. Apart from the decrease sometime between April and August the change is positive for all river basins the entire year.

Looking at the size of the average spring peak inflow the change for Lule and Skellefte is +/- 10 % compared to observations. For Dal it is a reduction with 0-50 %. Dal results for snowpack versus inflow during the second time period show how drastically the flow regime may be altered in the future. In all HADCM and two out of four of the ECHAM results the snowpack has almost completely disappeared and the spring peak in annual inflow has been evened out over the year.

7.6 Bias correction methods

Looking at the bias correction methods the choice of method can have a great impact on the result. MV, MVV and QM all have the ability to capture future changes in amount of dry days. However MV and MVV does not correct for the drizzle and overestimate the amount of rainy days compared to observed with 15-40 %.

QM corrects for number of dry days, it corrects extreme precipitation and it is sensitive. DC does not correct for number of dry days, but it keep the number of dry days from the

observed precipitation. It is also easy to use and gives a result that can be related to observed values. MV and MVV are not recommended due to the fact that the two methods indicate too many rain events and that extreme events are poorly calculated.

8 Conclusions

Precipitation will increase in the future. Change is greater in HADCM than ECHAM.

The total amount of inflow will increase towards the end of the century for both Lule and Skellefte and maximum snowpack decrease in the future for all river basins. Results indicate the increase in inflow is generally greater the further north the catchment is located and the majority of increase occurs during August - March.

Spring inflow (week 16-28) will increase in Lule and decrease in Skellefte and Dal. Spring peak inflow will remain relatively constant in Lule and Skellefte and decrease in Dal.

Results indicate an earlier spring flood in Dal for both time periods and in Lule and Skellefte mostly for the second. For Dal the accumulation of snow during winter almost stops entirely during the second time period leading to a radically changed flow regime. Spring flood for Dal the second time period is almost gone and inflow is relatively evenly distributed over the year.

Temperature will increase in the future with 0.3 - 4.5 degrees. For DC, MV and MVV the amount of change could mostly be attributed to which GCM was used. QM results for the second time period stood apart and showed similar results for both GCMs.

Looking at the individual bias correction methods QM and DC had the most reasonable results for amount of rainy days. In addition QM also had the ability to capture future changes in the amount of dry days.

QM showed the greatest interval difference in change of precipitation and the highest extreme event values. This indicated that the individual correction factors calculated by QM and two different polynomial functions they are fitted to had a clear impact on the end result.

QM results for temperature were the only ones where the choice of bias correction method had greater impact on the results than choice of GCM. This indicated the linear regression approach employed by QM has a clear impact on the results.

Overall it is our opinion that QM performed best and would be our recommendation for any application that didn't focus solely on the mean changes. If only the mean changes in amount of precipitation was of interest DC would be the best choice due to its simplicity.

9 Recommendations and limitations

To get results where the different bias correction methods would be possible to distinguish and overview the amount of emission scenarios, GCMs and RCMs were kept at a minimum. All of the above limit the scope of the results for the future predicted inflow to the hydropower system.

Important to mention is that bias correction methods are only responsible for a part of the uncertainties related to all predictions of future climate. Graham et. al., (2007) concluded that using different RCMs with the same GCM forcing and emission scenarios results in similar hydrological trends. He also concluded choice of GCM has a greater impact on the projected hydrological change than both choice of RCM and emission scenario. Kjellström et. al., (2010) draw similar conclusions that the spread of the result is largely depending on choice of GCM, and also that the choice of emission scenario starts to have a real impact mostly during the later decades of the century. This was also concluded by the IPCC, (2007) saying that choice of emission scenario has little effect for the first part of the century (2011 – 2030), more effect during the middle (2046-2065) and larger during the last decade (2090-2099).

These results are therefore only part of a wider range of possible future changes that would arise mainly from including more different global climate models and for the end of century also emission scenarios. A recommendation would therefore be to make a second study with the sole purpose of studying the future change in hydrological situation in Sweden due to climate change, and include several global emission scenarios and GCMs and only one RCM and QM for bias correction method. This would give results that incorporated a wider range of possible futures.

Looking at some parts of the result, for example total inflow and spring inflow it may seem a bit unlikely that such a big part of the change occurs already for the first time period, until 2040. An example is Lule drainage basin where the total inflow results show an increase of 30 % during the 25 years leading up to 2040 compared to observed. The second time period shows and increase of up to 40 % compared to observed which would mean that from 2040 and during the remainder of the century it would increase 10 more %. This could indicate that especially HADCM overestimates the precipitation increase for the first part of the century. It would be interesting to compare this to results from other GCMs and see how they differ compared to the ECHAM and HADCM results, and also look at what happens during 2040-2076.

10 References

Andréasson J, Bergström S, Carlsson B, Graham L P, and Lindström G, 2004. Hydrological change – climate change impact simulations for Sweden. *Ambio* volume 33 page 228-234.

Bergström S, Andréasson J, Beldring S, Carlsson B, Graham L P, Jónsdóttir J F, Engeland K, Turunen M A, Vehviläinen B and Förland E J, 2003. Climate change impacts on hydropower in the northern countries - state of the art discussion of principles. Rejkjavik, Iceland, CWE Hydrological Models Group: 36.

DHI, 2011. Powerpoint presentation prepared by DHI to showcase the quantile mapping bias correction method

Gordon C, Cooper C, Senior C A, banks H, Gregory J M, Johns T C, Mitchell J F B, Wood R A, 1999. The simulation of SST, sea ice extents and ocean heat transports in a version of the Hadley centre coupled model without flux adjustments. *Climate dynamics* volume 16, page 147-168.

Google.maps.se, 2012. Available at: http://maps.google.se/ [Accessed 2012-05-19]

Graham L. Phil., Andreasson J, Carlsson B, 2007. Assessing climate change impacts on hydrology from an ensemble of regional climate models, model scales and linking methods - a case study on the Lule River basin. *Climate change* Vol 81, page 293-307.

IPCC, n.d. *Intergovernmental Panel on Climate Change – Organization* Available at: http://www.ipcc.ch/organization/organization.shtml [Accessed 16 January 2012]

IPCC, 2000. *IPCC special report – emission scenarios*. ISBN: 92-9169-113-5.

IPCC, 2007. Climate change 2007: The physical science basis. *Contribution of Working Group I to the Fourth Assessment Report of the Intergovernmental Panel on Climate Change*. Cambridge university press, New York.

IPCC, 2011. Data Distribution Center - Carbon Dioxide: Projected emissions and concentrations. Available at: http://www.ipcc-data.org/ddc_co2.html [Accessed 30 May 2012]

Kjellström E, Nikulin G, Hansson U, Strandberg G, Ullerstig A, 2010. *21st changes in the European climate: uncertainties derived from an ensamble of climate model simulation*. Rossby Centre and Swedish Meteorological and Hydrological Institute. Norrköping, Sweden.

Kleinn J. Frei C, Gurtz J, Luthi D, Vidale PL, Schar C, 2005. Hydrologic simulations in the Rhine basin driven by regional climate model. *JOURNAL OF GEOPHYSICAL RESEARCH-ATMOSPHERES* Volume: 110 Issue: D4 Article Number: D04102

Lawrence D, Haddeland I, Langsholt E, 2009. Calibration of HBV hydrological models using PEST parameter estimation. Norweigian Water Resources and Energy Directorate, Oslo.

Madsen H, Sunyer M A. , Yamagata K (2010) Climate change impact assessment on water resources in North-Easr Sealand, Denmark- Comparison of statistical downscaling methods

Max Planck institute of meteorology, 2003. *The atmospheric general circulation model ECHAM5*. Available at: http://www.mpimet.mpg.de/fileadmin/publikationen/Reports/max_scirep_349.pdf

Meehl G A et al, 2007. The Global Climate Projections, in *Climate Change 2007: The Physical Science BasisContribution of Working Group 1 to the Fourth Fourth Assessment Report of the Interngovernmental Panel on Climate Change*. Page 747-845, Cambridge university press, Cambridge, U.K.

Piani C, Haerter J O and Coppola E, 2010. Statistical bias correction for daily precipitation in regional climate models over Europe. *Theoretically Applied Climatology*, volume 99 page 187-192.

Samuelsson P, Jones C G, Wilén U, Ullerstig A, Gollvik S, Hansson U, jansson C, Kjellström E, Nikulin G, Wyser K, 2010. The Rossby Centre Regional Climate model RCA3: model description and performance. *Tellus* volume 63A page 4-23.

SMHI, 2009 *HBV* (2009-04-08) Available at: http://www.smhi.se/forskning/forskningsomraden/hydrologi/hbv-1.1566 [Accessed 2012-05-25]

SMHI, 2010 FAKTABLAD NR 44 – *Sveriges vattendrag* Available at: http://www.smhi.se/polopoly_fs/1.10713!webbSveriges%20vattendrag%2016.pdf [Accessed 2012-05-09]

Stute M, Clement A, Lohmann G, 2011. Global climate models: Past, present and future. *Proceedings of the National Academy of Sciences of the United States of America*, Vol 98, page 10529-10530.

Svenskenergi, 2011. *Elåret 2010* [online] (2011-09-12) Available at: http://www.svenskenergi.se/upload/Statistik/Elåret/fickfolder-statistik2010.pdf [Accessed 2012-01-17]

Swedish energy agency, 2008. *Extrema väderhändelser och klimatförändringens effekter på energisystemet*. ER 2009:33

Van Roosmalen, L. 2009. The effects of future climate change on groundwater and stream discharge in Denmark. Ph.D. diss. Dep. Of Geography and Geology, Univ. of Copenhagen.

Van Roosmalen L, Sonnenborg T.O, Jensen K.H, Christensen J.H (2011) Comparison of hydrological Simulations of Climate Change Using Perturbation of Observations and Distribution-Based Scaling, *VADOSEZONE JOURNAL* Volume: 10 Issue: 1 Pages: 136-150

Vattenmyndigheterna, n.d.(1) *Luleälvens avrinningsområd* (n.d) Available at: http://www.vattenmyndigheterna.se/SiteCollectionDocuments/sv/bottenviken/publikationer/beskrivning-haro-kustmynnande/haro9-lulealven.pdf [Accessed 2012-01-14]

Vattenmyndigheterna, n.d.(2) *Skellefteälvens avrinningsområd* (n.d) Available at: http://www.vattenmyndigheterna.se/SiteCollectionDocuments/sv/bottenviken/publikationer/beskrivning-haro-kustmynnande/20-skelleftealven.pdf [Accessed 2012-01-14]

Viss.lansstyrelsen.se, n.d. *Vattenkartan – Länsstyrelsens WebbGIS* Available at: http://www.viss.lansstyrelsen.se/MapPage.aspx [Accessed 2012-05-10]

Wetterhall F, Graham L. P, Andréasson J, Rosberg J, Yang W (2011) Using ensemble climate projections to assess probabilistic hydrological change in the Nordic region, *NATURAL HAZARDS AND EARTH SYSTEM SCIENCES*
Volume: 11 Issue: 8 Pages: 2295-2306

Yang W, Andreasson J, Graham L P, Olsson J, Rosberg J, and Wetterhall F, 2010. Distribution-based scaling to improve usability of regional climate model projections for hydrological climate change impacts studies. *Hydrology Research*, volume 41 section 3-4.

Österberg K & Eriksson L, 2004. Lönsamt spana efter vårfloden, *Ny Teknik*